

Article

Stochastic Fractal Search Optimization Algorithm Based Global MPPT for Triple-Junction Photovoltaic Solar System

Hegazy Rezk^{1,2,*}  and Ahmed Fathy^{3,4} 

¹ College of Engineering at Wadi Addawaser, Prince Sattam Bin Abdulaziz University, Wadi Addawaser 11991, Saudi Arabia

² Electrical Engineering Department, Faculty of Engineering, Minia University, Minia 61517, Egypt

³ Electrical Engineering Department, Faculty of Engineering, Jouf University, Sakaka 72314, Saudi Arabia; afali@zu.edu.eg

⁴ Electrical Power and Machine Department, Faculty of Engineering, Zagazig University, Zagazig 44519, Egypt

* Correspondence: hr.hussien@psau.edu.sa

Received: 28 August 2020; Accepted: 17 September 2020; Published: 22 September 2020



Abstract: A significant growth in PV (photovoltaic) system installations have been observed during the last decade. The PV array has a nonlinear output characteristic because of weather intermittency. Partial shading is an environmental phenomenon that causes multiple peaks in the power curve and has a negative effect on the efficiency of the conventional maximum power point tracking (MPPT) methods. This tends to have a substantial effect on the overall performance of the PV system. Therefore, to enhance the performance of the PV system under shading conditions, the global MPPT technique is mandatory to force the PV system to operate close to the global maximum. In this paper, for the first time, a stochastic fractal search (SFS) optimization algorithm is applied to solve the dilemma of tracking the global power of PV system based triple-junction solar cells under shading conditions. SFS has been nominated because it can converge to the best solution at a fast rate. Moreover, balance between exploration and exploitation phases is one of its main advantages. Therefore, the SFS algorithm has been selected to extract the global maximum power point (MPP) under partial shading conditions. To prove the superiority of the proposed global MPPT–SFS based tracker, several shading scenarios have been considered. The idea of changing the shading scenario is to change the position of the global MPP. The obtained results are compared with common optimizers: Antlion Optimizer (ALO), Cuckoo Search (CS), Flower Pollination Algorithm (FPA), Firefly-Algorithm (FA), Invasive-Weed-Optimization (IWO), JAYA and Gravitational Search Algorithm (GSA). The results of comparison confirmed the effectiveness and robustness of the proposed global MPPT–SFS based tracker over ALO, CS, FPA, FA, IWO, JAYA, and GSA.

Keywords: optimization; modelling; renewable energy; triple junction solar cell; shading condition; energy efficiency

1. Introduction

Due to the environmental impact of fossil fuels that currently act as our main energy source [1], there is a rapid growth in the usage of renewable energy as an alternative energy source [2–4]. Thanks to the reduction in the cost of renewable energies such as biomass [5–7], solar thermal [8], and solar PV (photovoltaic) energies [9], wind energy [10], their application is becoming more widespread. Among different renewable energies, the PV system is a promising energy source for sustainable progress [11]. Photovoltaic solar panels are considered the most widely used source of renewable energy around the world. Their produced energy is clean, pollution-free, and eco-friendly [12]. They have spread

worldwide in the past few years due to their price reduction, their relatively long lifespan, and their low maintenance requirements. Unfortunately, conventional photovoltaic panels suffer a major drawback, which is efficiency. In fact, a solar panel converts between 12 and 18 percent of the solar energy depending on the type of solar panel, into electric energy, the remaining 82 to 88 percent of the solar energy is converted into heat which increases the temperature of the surface of the solar panel.

The improvement of PV efficiency is a great challenge to most researchers especially in case of operating under partial shadow conditions. Moreover, most of them recommend new materials with high efficiency of conversion to enhance the PV performance. Many technologies have been employed in manufacturing the PV cell like mono-crystalline, poly-crystalline, multi-crystalline, and ribbon multi-crystalline [13]. Additionally, there are thin-film technologies like amorphous silicon, cadmium telluride (CdTe), and copper-indium-gallium-diselenide (CIGS) are manufactured.

Recently, a great interest was devoted to multi-junction solar cells (MJSC) [14,15], which comprises different PV junctions stacked over one another via homojunctions, intrinsic materials or tunnel junctions.

Each solar cell has a different bandgap energy, MJSC is characterized by its efficiency in capturing and converting a large amount of photon wavelengths to electrical power. Motivated by efficient performance, MJSCs have received much attention especially for concentrating PV systems (CPVs). MJSCs have high conversion efficiencies with a value more than 40% [16]. CPVs are considered as one of the most promising research avenues that help in decreasing the cost of solar energy, especially in large scale applications. Today, the concentrated PV panels are mostly based on MJSCs made up of several p-n junctions interconnected in series, typically a GaInP/GaInAs/Ge topology [17]. MJSCs used in concentrated PV systems are different from silicon type cells, they are capable of capturing and converting large amounts of sunlight into electrical energy with high efficiency [13]. Or and Appelbaum studied the effect of temperature and concentration on the InGaP/GaAs/Ge MJSC parameters. Based on the calculated parameters, the performance of InGaP/GaAs/Ge MJSC and concentrated PV array under different operating conditions may be identified [18]. Two concentrator modules have been investigated by Fernández et al. [17] under controlled conditions with the aid of a CPV solar simulator under light intensity in the range of 700–1000 W/m². The authors concluded that, the photo-generated current is dependent on the irradiance, while the ideality factor and saturation current are stable under variable irradiances. Moreover, the parasitic resistances (series and parallel) are decreased when the intensity is increased. Segev et al. [19] presented different models of triple-junction solar cells (TJSCs) compared with experimental data under variable flux concentration and temperature. Single and two diode-based models presented root mean square error (RMS) errors of less than 2.5%.

To enhance the PV system efficiency, the maximum power point tracking (MPPT) approach must be considered. The PV system has a nonlinear output characteristic owing to weather intermittency. Therefore, an efficient MPPT which is not only high in efficiency but also enhances the PV output power, is expected to be designed [13,20]. Under uniform solar irradiance, the voltage versus power curve contains a unique maximum power point (MPP). This point can be easily extracted using different conventional tracking methods like perturb and observe (P&O), hill-climbing, and incremental conductance (INC). However, the situation is completely different under shading conditions when the solar panel receives non-uniform irradiance. The partial shading generates multiple peaks in the curve of output power and has negative effects on the conventional MPPT methods' efficiency [21].

It is known that, the current flow through series connected cells is constant, therefore, the shaded cells try to operate with reverse bias voltage to give the same current of the illuminated ones. However, power consumption is placed due to the reverse power polarity, this causes weakening in the maximum generated power. Moreover, hotspots are generated due to excessive reverse bias voltage. This can be solved via connecting bypass diode to certain cells [21]. The PV array characteristics with bypass diodes are different than those of a conventional array without these diodes. Since the bypass diodes generate a path of alternate current, cells of a module do not have the same current, in case of operation under partial shadow. Therefore, the power–voltage (P–V) curve has multiple maxima as shown in

Figure 1. This figure confirms the difference between the characteristics of PV array with and without bypass diodes. Most conventional MPPT algorithms failed in distinguishing between the local and global maximum power in the P–V curve of the partially shaded PV array.

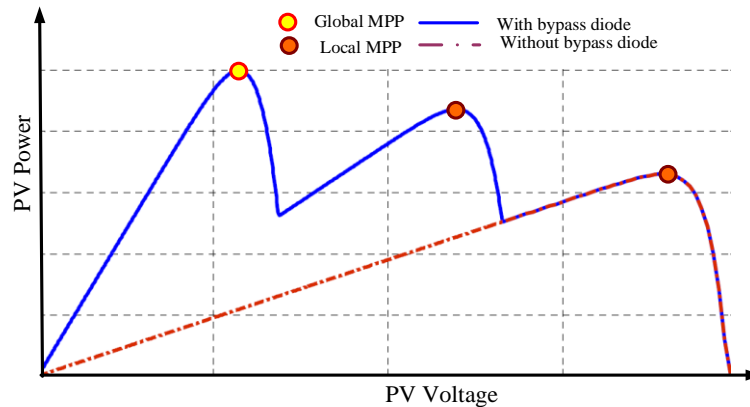


Figure 1. PV (photovoltaic) array power–voltage (P–V) characteristic under partial shading condition.

A new MATLAB/Simulink model of TJSCs has been suggested by Rezk and Hasaneen [16]. The proposed model has been integrated with MPPT based on artificial neural networks (ANN). The proposed MPPT technique increased energy by 11.28%. The drawback of this work is that it cannot handle the shading condition. A hybrid MPPT method for partially shaded PV arrays is suggested by El-Helw et al. [22]. The presented hybrid technique integrated an artificial neural network and a conventional P&O method. This method can be considered costly since the control system needs four sensors: temperature, irradiance, voltage, and current. Moreover, there is an additional drawback of the dependency of the characteristics of the PV module. An attempt to reduce the number of sensors of the MPPT controller has been done by Rezk [23]. The proposed strategy is based on only a single current sensor. Several shading scenarios were considered to prove the reliability of the presented global MPPT. The essential limitation of this method its validity only for battery charger applications. Engel et al. [24] suggested a global MPPT based on an antlion optimizer (ALO). The size of the population considered in that work is selected to be 40, which is considered extremely high and time-consuming. Moreover, only one shading scenario is considered and compared with conventional P&O. In the same direction, Sahu and Shaw [25] used the same optimizer to track the global MPP. They did not use ALO to track the global MPP directly, but it has been employed to determine the optimal parameters of the PID (proportional–integral–derivative) controller. Additionally, only one shading scenario is considered and compared with conventional P&O. A drawback of such a method, is the requirement of an additional voltage sensor (load voltage). These issues have been solved by Kumar et al. [25]. Five different shading scenarios are considered. Subha and Himavathi [26] proposed a flower pollination algorithm (FPA) to solve the problem of shading conditions. Ten different shading scenarios are used to investigate the performance of FPA. The obtained results are compared with particle swarm optimization (PSO). Approximately two seconds are required to extract the global MPP. A summary of some selected previous MPPT methods is presented in Table 1.

In this research, a novel algorithm called Stochastic Fractal Search (SFS) is proposed to extract the global power of a partially shaded PV system employing a triple-junction solar cell. To prove the superiority of the proposed global MPPT–SFS based tracker, several shading scenarios have been considered. The idea of changing the shading scenario is to change the position of the global MPP. The obtained results are compared with common optimizers including: the Antlion Optimizer (ALO), Cuckoo Search (CS), Flower Pollination Algorithm (FPA), Firefly-Algorithm (FA), Invasive-Weed-Optimization (IWO), JAYA and Gravitational Search Algorithm (GSA). The obtained results confirmed the competence and robustness of the proposed SFS–MPPT in extracting the global maximum power from the TJS based system. The rest of this paper is summarized as follows: the next

section describes the modeling of a multi-junction solar cell-based PV module. Section 3 presents a brief description of stochastic fractal search optimization algorithms. The results and discussions with the performance of proposed SFS are shown in Section 4. Finally, the last section provides conclusions.

Table 1. Summary of some selected previous maximum power point tracking (MPPT) methods.

Author	Type Of PV Cell	MPPT Method	PV Array Dependency	Required Sensors	Control Parameter	Implementation	Handling Partial Shading
Das et al. [27]	Triple-junction InGaP/GaAs/Ge	Perturb and observe (P&O)	NO	Current and voltage	Duty cycle	Matlab software	NO
Rezk and Hasaneen [16]	InGaP/InGaAs/Ge triple-junction solar	Artificial neural network (ANN)	YES	Temperature, radiation, and voltage	PV voltage	Matlab software	NO
El-Helw et al. [22]	Not mentioned	Hybrid ANN and P&O	YES	Temperature, radiation, voltage and current	PV voltage	Matlab software	YES
Engel et al. [24]	Not mentioned	Ant Lion Optimization (ALO)	NO	Voltage and current	Duty cycle	Matlab software	YES
Sahu and Shaw [25]	Not mentioned	ALO	NO	Two voltage sensors and one current sensor	-	Matlab software	YES
Kumar et al. [25]	Solar PV simulator	ALO	NO	Voltage and current sensor	Duty	experimental	YES
Subha, and Himavathi [26]	Not mentioned	Flower Pollination Algorithm (FPA)	NO	Voltage and current	PV voltage	Matlab software	YES
Diab and Rezk [15]	Multi-crystalline silicon cell	FPA	NO	Voltage and current	Duty cycle	Matlab software	YES
Ram and Rajasekar [28]	Polycrystalline solar cell	FPA	NO	Voltage and current	Duty cycle	Experimental and Matlab software	YES
Ajjatmo and Robandi [29]	Not mentioned	FPA	NO	Voltage and current	Duty cycle	Co-simulation PSIM and Matlab	YES
Rezk [23]	Not mentioned	Particle Swarm Optimization (PSO)	NO	Only single current sensor	Duty cycle	Matlab simulation	YES
Eltamaly [30]	Not mentioned	Improved PSO	NO	Voltage, current, and number of radiation sensors	Duty cycle	Matlab simulation	YES
Omar et al. [31]	Monocrystalline Silicon	Incremental conductance (INC) tuned by Invasive Weed Optimization (IWO)	NO	Voltage and current	Duty cycle	Matlab simulation	NO
Li et al. [31]	Not mentioned	Gravitational Search Algorithm (GSA)	YES	Three temperature sensors and three irradiance sensors	PV voltage	Matlab simulation	YES

Table 1. Cont.

Author	Type Of PV Cell	MPPT Method	PV Array Dependency	Required Sensors	Control Parameter	Implementation	Handling Partial Shading
Huang et al. [32]	PV simulator	JAYA	NO	Voltage and current	PV voltage	Experimental	YES
Nguyen et al. [33]	Monocrystalline	Modified P&O	NO	Voltage and current	Duty cycle	Matlab simulation and Experimental	No
Xu et al. [34]	Polycrystalline	Modified INC	NO	Voltage and current	Duty cycle	Simulation	NO
Mohamed et al. [35]	Monocrystalline	Grey Wolf Optimization	NO	Voltage and current	Duty cycle	Matlab simulation	YES
Omer et al. [36]	Monocrystalline	Wind driven optimization	NO	Voltage and current	Duty cycle	Matlab simulation	YES
Li et al. [37]	PV simulator	Fuzzy-logic	NO	Voltage and current	Duty cycle	Matlab simulation and Experimental	YES
Pilakkat et al. [38]	Polycrystalline	Improved P&O	NO	Voltage and current	Duty cycle	Matlab simulation	YES
Sai et al. [39]	Not mentioned	Improved SuDoKu	NO	Voltage and current	Duty cycle	Matlab simulation	YES

2. Multi-Junction Solar Cell-Based PV Module

The TJSC equivalent circuit includes the parameters of each sub-cell. Moreover, the effect of temperature variations on the gap energy and the reverse saturation currents for each cell are also included. The single-diode model of the PV cell comprises a light-current with an anti-parallel diode, one resistor in shunt, and a resistor in series. The single-diode circuitry for a triple-junction InGaP/InGaAs/Ge solar cell is represented in Figure 2 [21].

The model comprises three sub-cells which are top, medium, and bottom. The energy gaps are reduced from top to bottom. The current extracted from the TJSC is formulated by the following Equation:

$$I_C = I_{Li} - I_{Di} - I_{shi} \quad \forall i = [1, 2, 3] \quad (1)$$

The light generated current can be expressed as follows:

$$I_{Li} = GK_C \left[I_{sci} + a(T - T_{Ref}) \right] \quad (2)$$

where T_{Ref} is the reference temperature in °C, a is the temperature coefficient of the short circuit current in A/°C, K_C is the ratio of concentration, and G is the solar radiation in W/m². The diode current, voltage drop, and saturation current can be written as follows:

$$I_{Di} = I_{Oi} \left[\exp\left(\frac{qV_{Di}}{A_i K_B T}\right) - 1 \right] \quad (3)$$

$$V_{Di} = V_i + I_C \times R_{Si} \quad (4)$$

$$I_{Oi} = K_i \times T^{(3 + \frac{\gamma_i}{2})} \left[\exp\left(-\frac{E_{gi}}{A_i K_B T}\right) \right] \quad \forall i = [1, 2, 3] \quad (5)$$

The TJSC terminal voltage can be expressed as follows:

$$V_C = \frac{n_1 K_B T}{q} \ln \left[\frac{I_{L1} - I_C}{I_{O1}} + 1 \right] + \frac{n_2 K_B T}{q} \ln \left[\frac{I_{L2} - I_C}{I_{O2}} + 1 \right] + \frac{n_3 K_B T}{q} \ln \left[\frac{I_{L3} - I_C}{I_{O3}} + 1 \right] - I_C \times R_S \quad (6)$$

where

$$R_S = R_{S1} + R_{S2} + R_{S3} \quad (7)$$

where q is the electron charge, n_i is the ideality factor of the diode, K_B is the constant of Boltzmann, E_g is the energy of bandgap, K and γ are constants, T is the absolute temperature, and R_S is the series resistance of the cell. The relationship between the bandgap energy and temperature can be expressed as [18]:

$$E_g(T) = E_g(0) + \frac{\alpha T^2}{T + \beta} \quad (8)$$

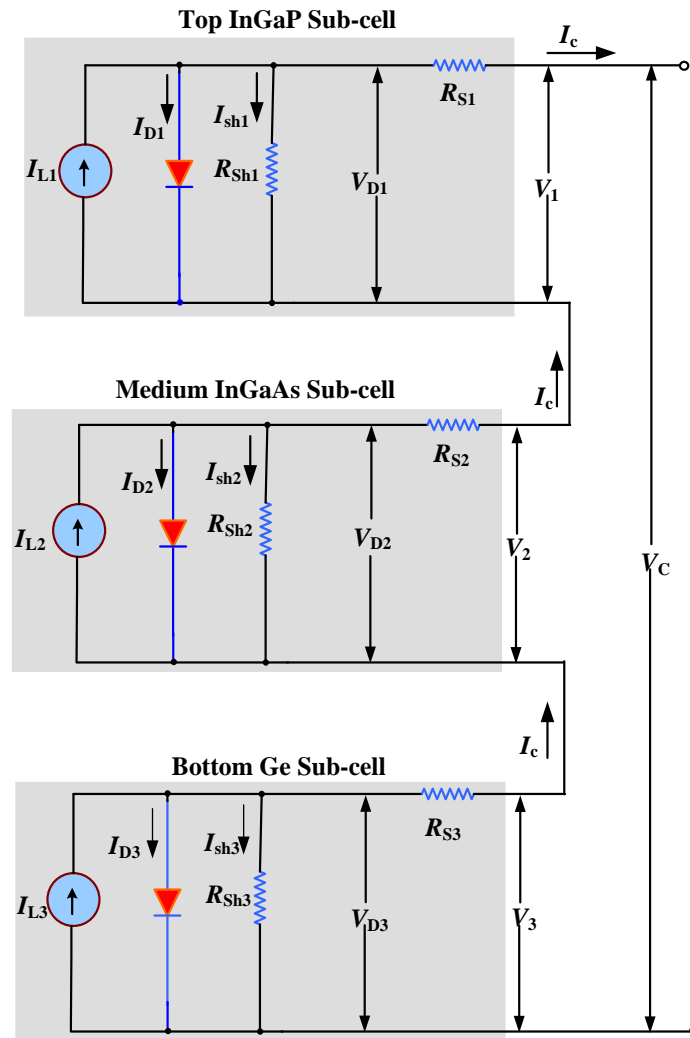


Figure 2. Model of triple-junction solar cell (TJSC).

3. Stochastic Fractal Search Optimization Algorithm

A stochastic fractional search (SFS) optimizer was presented by Salimi [40] and motivated from the growth phenomenon. In such approach, the diffusion limited aggregation (DLA) concept is employed to initiate random fractal growth. Two phases are followed in implementing SFS—the diffusion and updating processes. In the diffusion process, each particle designated has potential energy, each particle spreads around its current location to improve the exploitation ability of the approach. This action distinguishes the approach from the others in avoiding getting stuck in local optima. In this phase, random new particles are created with the aid of Levy flight and Gaussian walk, a few of them continue

in generation while the rest are ignored. Moreover, SFS uses some random updates that lead to exploration properties. Firstly, each particle is located randomly based on the following formula:

$$E_i = \frac{E}{P} \quad (9)$$

where E_i is the energy of particle P_i , E is the maximum considered potential energy and P is the number of particles. Levy flight and Gaussian walk are employed in SFS to simulate the generation of new particles, this can be expressed as follows:

$$x_i^q = x_i + \alpha_i^q \otimes Levy(\lambda) \quad (10)$$

$$x_i^q = x_i + \beta \cdot Gaussian(P_i, |BP|) - (\gamma \cdot BP - \gamma' \cdot P_i) \quad (11)$$

where α is the factor of distribution scale, β denotes the distribution index in range of $[0, 2]$, q is the number of generated particles developed from the main particle diffusion, x_i is the current position of i^{th} particle, $Gaussian(P_i, |BP|)$ is the Gaussian distribution with mean of P_i and standard deviation of BP which denotes the best position, γ and γ' are random numbers in range $[0, 1]$. To improve the convergence rate of the SFS optimizer, two formulas of the parameter α are used, one of them is employed for searching in a wide space while the other is for evaluating the solution with high precision. The two formulas of α are as follows:

$$\alpha_i = \frac{\log(\min(\hat{E}))(U_b - L_b)}{g \cdot \log(E_i)} \quad (12)$$

$$\alpha_i = \frac{(U_b - L_b)}{(g \cdot \log(E_i))^\psi} \quad (13)$$

where $\min(\hat{E})$ is the minimum energy in the search space, U_b and L_b are the search space upper and lower bounds, g is the number of iterations, E_i is the energy of P_i particle and ψ is a fixed value of 1.5. After diffusion process, the energy of the main particle is divided among the new generated particles according to the following formula:

$$E_i^j = \left[\left(\frac{f_i}{f_i + \sum_{k=1}^q f_k} \right) \right] \cdot E_i \quad (14)$$

where f_i is the value of the main particle fitness. As stated before, not all the particles continue in generating new ones, few of them are considered and the others are ignored. The remaining particles energy equation can be written as follows:

$$E_{new}^t = E_{old}^t + \left[\left(\frac{f_t}{\sum_{k=1}^{\xi} f_k} \right) \cdot \varphi \right] \cdot \mu \quad (15)$$

where φ is the total energy of the ignored particles and μ is the energy distributing rate between the considered and generated particles and ξ is the number of particles in the iteration. In SFS, diffusion limited aggregation (DLA) methodology is responsible for inspiring random growth process, this is done via random walk only, with the aid of Gaussian distribution as follows:

$$GW_1 = Gaussian(\mu_{BP}, \sigma) + (\varepsilon \cdot BP - \varepsilon' \cdot P_i) \quad (16)$$

$$GW_2 = \text{Gaussian}(\mu_P, \sigma) \quad (17)$$

where ε and ε' are random numbers in range $[0, 1]$, μ_{BP} , μ_P and σ are the gaussian parameters, μ_{BP} is equal to $|BP|$ while μ_P is equal to $|P_i|$. The standard deviation can be calculated as follows:

$$\sigma = \left| \frac{\log(g)}{g} \cdot (P_i - BP) \right| \quad (18)$$

where the term $(\log(g)/g)$ is employed for reducing the Gaussian walks during increasing the generations' number. The particles are initialized as follows:

$$P_j = L_b + \varepsilon \cdot (U_b - L_b) \quad (19)$$

After that, the fitness function of each particle is evaluated and the best point (BP) is obtained. All particles move around their current positions to exploit the search space of the problem. Additionally, two statistical measures are employed to enhance the exploration, the first one is applied on each individual while the second one is applied on all particles. The first statistical measure is applied by sorting all points according to their fitness functions and then calculating the probability assigned to each individual according to the following expression:

$$Pa_i = \frac{\text{rank}(P_i)}{N} \quad (20)$$

where $\text{rank}(P_i)$ is the particle P_i rank in the group and N is the total number of points in the population. Referring to Equation (20), larger probability will be assigned to the higher ranked individual. Additionally, it is employed to increase the chance of changing the points that did not get good solutions. The j^{th} component of individual P_i is updated as follows:

$$P_i'(j) = P_r(j) - \varepsilon \cdot (P_t(j) - P_i(j)) \quad \text{if } Pa_i < \varepsilon \quad (21)$$

where P_i' is the modified position of P_i , P_r and P_t which are selected randomly in the group. The changing position of a point with respect to the others is the target of the second statistical change. This action is done for the purpose of improvement the exploration quality. If $Pa_i < \varepsilon$, the positions of P_i' is updated according to Equations (22) and (23) otherwise, no amendment will be made.

$$P_i'' = P_i' - \varepsilon \cdot (P_t' - BP) \quad |\varepsilon' \leq 0.5 \quad (22)$$

$$P_i'' = P_i' - \varepsilon \cdot (P_t' - P_r') \quad |\varepsilon' > 0.5 \quad (23)$$

where P_i' , P_r' and P_t' are selected randomly based on Equation (21), ε are random numbers generated via Gaussian distribution. Updating process between P_i' and P_i'' is performed in case of improving in fitness function. Figure 3 shows the flow chart of the SFS optimizer.

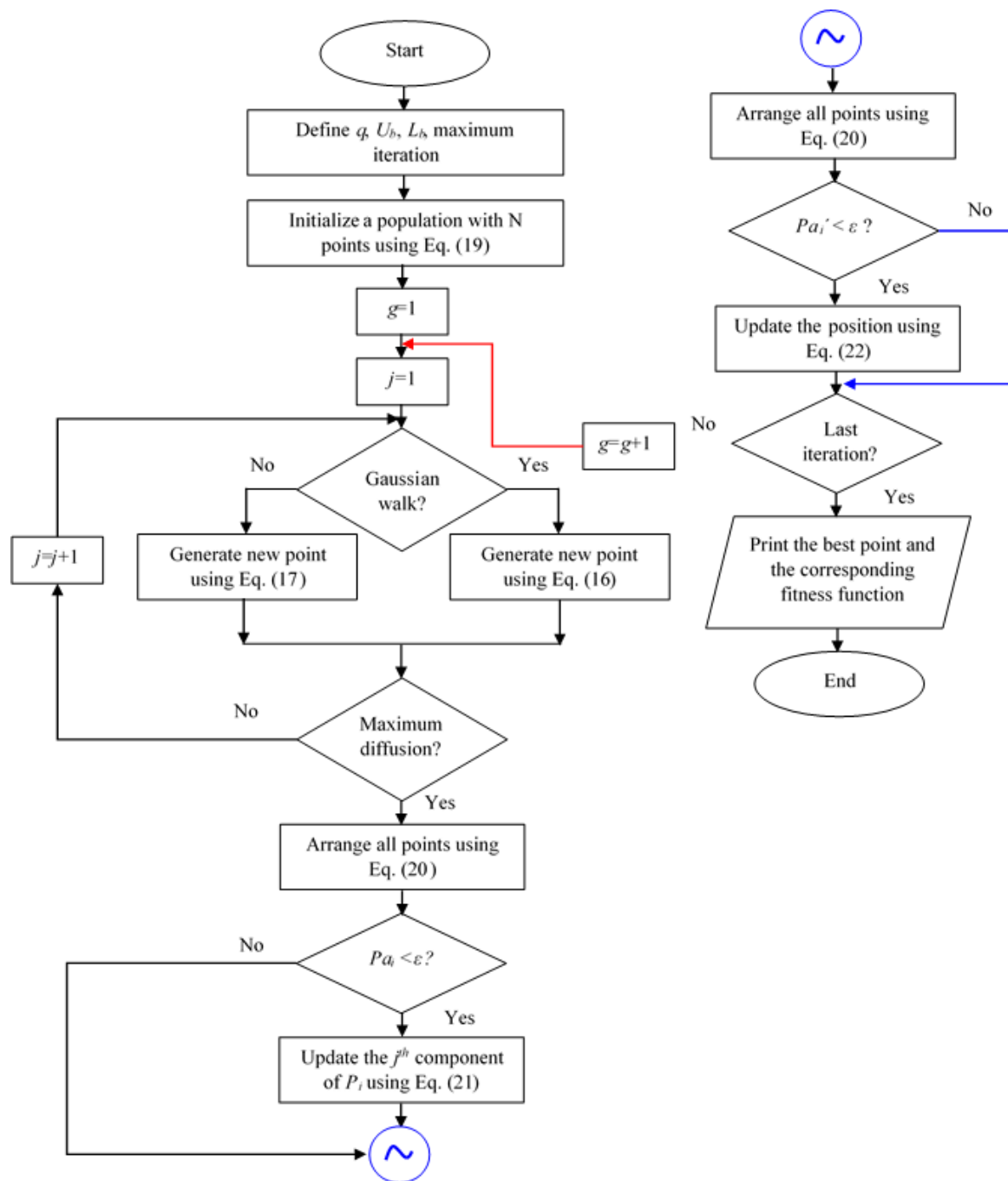


Figure 3. Flowchart of the optimization process of stochastic fractal search (SFS) optimizer.

4. Results and Discussion

To prove the superiority and reliability of the proposed strategy, an extensive simulation under different shading scenarios was carried out using Matlab/Simulink. To illustrate the supremacy of the proposed technique, the obtained results are compared with those obtained via ALO, CS, FPA, FA, IWO, JAYA and GSA methods. The performance of different MPPT methods is analyzed concerning the success rate (SR), standard deviation (StD), coefficient of variation, average relative error (RE), mean absolute error (MAE), root mean square error (RMSE), efficiency, population variance, minimum value and average value under each shading pattern. Three configurations: two modules in series, three modules in series and four modules in series are considered. For every configuration, two different shading scenarios are implemented and investigated. Moreover, six shading patterns, which includes

different shading effects, were considered in the present work. The shading patterns considered to have different global MPP positions, such as first, second, and third peaks. Table 2, Figures 4 and 5 illustrate the detailed description of different considered shading scenarios.

Table 2. The detailed description of different considered shading scenarios. MPP: maximum power point.

Scenario Number	Solar Irradiance Levels Distribution on Modules W/m ²	Voltage at MPP, V	Current at MPP, A	Local and Global MPP, W			Position of Global Maximum Power Point (GMPP)	
1	1,000,700	103.83	9.60	571.30	996.59		Right	
2	1,000,300	42.81	13.34	571.30	438.80		left	
3	1,000,800,600	163.48	8.27	571.30	1129.00	1351.40	1st right	
4	1,000,800,200	102.94	10.97	571.30	1129.40	465.90	center	
5	1,000,700,400,200	103.83	9.60	571.30	996.59	907.10	2nd left	
6	1,000,800,600,400	163.48	8.27	571.30	1129.4	1351.40	12,320	2nd right

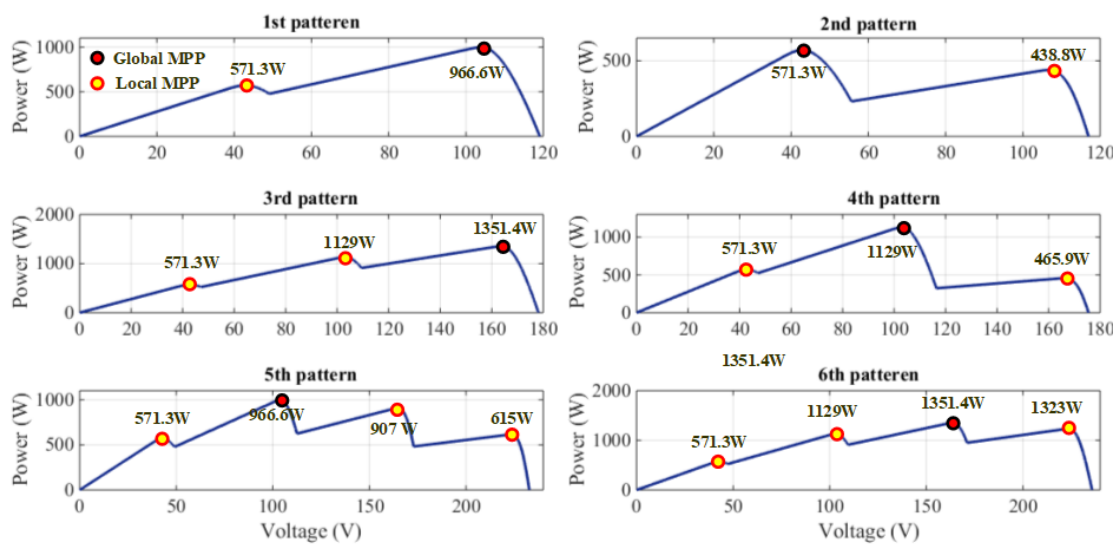


Figure 4. The P–V curves of the studied PV systems with different shadow patterns.

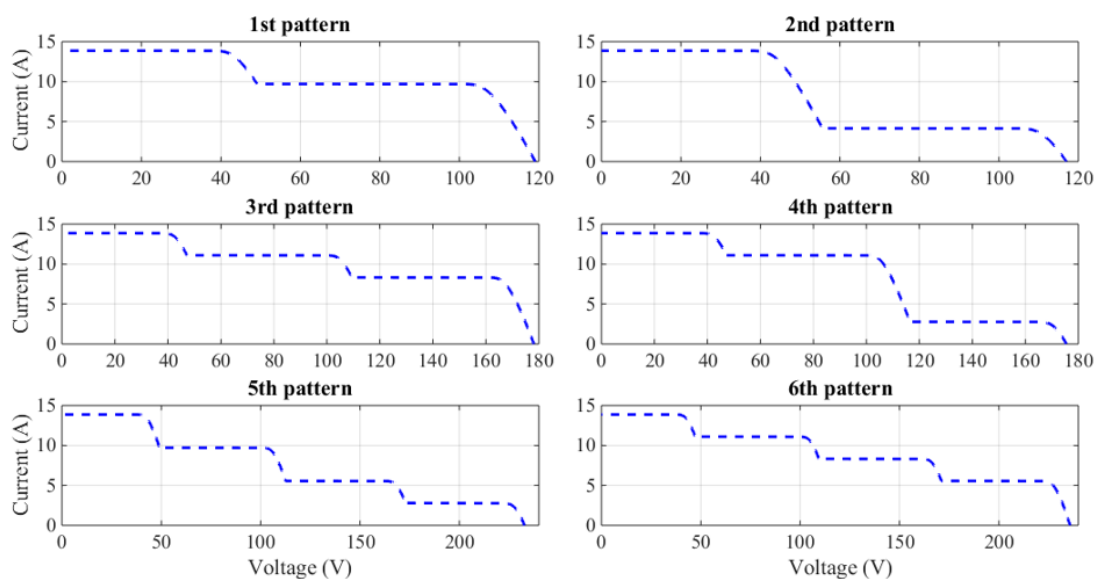


Figure 5. The current-voltage (I–V) curves of the studied PV systems with different shadow patterns.

The first shading scenario is applied to the first PV configuration where two series PV modules are connected in series. The solar irradiance levels distribution on the two PV modules are 1000 W/m^2 and 700 W/m^2 , respectively. Under this condition, there are two peaks. The local and global power values are 571.3 W and 996.59 W , respectively. The global maximum power is located at the right side of the power–voltage curve. The corresponding PV voltage and current at global power are 103.83 V and 9.60 A , respectively.

Throughout the first shading scenario, the best success rate values are archived by SFS and FA optimizers while the worst rate is assigned to ALO. Out of 50 runs, SFS cannot extract the minimum benchmark of global power (986 W) three times: run#24, run#41 and run#44. Twenty-one times ALO did not reach to the global power. A summary of the evaluation of the statistical performance of different considered global MPPT methods is presented in Table 3. More details about the extracted power of each optimizer are shown in Table A1. The minimum standard deviation of 4.11 is achieved by SFS followed by FA whereas the largest value of 135.23 is assigned to CS optimizer. Additionally, the minimum RMSE of 4.34 is achieved by SFS. In sum, for first shading scenario SFS optimizer performed the best compared with other methods.

The second shading scenario is also applied to the first PV configuration. The solar irradiance level applied to the first PV module is kept same as the first scenario where the radiation level subjected to the second PV module is decreased from 700 W/m^2 to 300 W/m^2 . This leads to transfer of the position of the global power from the right position to the left. This is very useful to investigate the reliability of the proposed SFS based tracker. The local and global power values are 438.8 W and 571.3 W , respectively. The corresponding PV voltage and current at global power are 42.81 V and 13.34 A . During the second shading scenario, the best success rate of 100% is achieved by SFS, followed by the FA optimizer (96%), while the worst rate of 60% is assigned to ALO. Out of 50 runs, ALO did not extract the global power twenty times, as presented in Table A1. The minimum standard deviation values are achieved by SFS and JAYA, whereas the largest value of 32.92 is assigned to the ALO optimizer. The same thing also occurred for the RMSE. This also confirms that the SFS optimizer performed the best compared with other methods.

The third shading scenario is applied to the second PV configuration where three series PV modules are connected in series. The solar irradiance levels distribution on the three PV modules are 1000 W/m^2 , 800 W/m^2 and 600 W/m^2 , respectively. Under this condition, there are three peaks: 571.3 W , 1129 W and 1351.4 W . The global maximum power is located at the right side of the power versus voltage curve. The corresponding PV voltage and current at global power are 163.48 V and 8.27 A .

The fourth shading scenario is also applied to the second PV configuration. The solar irradiance levels applied to the first and second PV modules are kept same as third scenario, where the radiation level subjected to the third PV module is decreased from 600 W/m^2 to 200 W/m^2 . This leads to transfer of the position of the global power from the right position to the middle. This is also done to test the reliability of the proposed SFS based tracker when the global power located at the center of the power–voltage curve. The local power values are 571.3 W and 465.9 W , whereas and global power value is 1129.4 W . The corresponding PV voltage and current at global power are 102.94 V and 10.97 A . Throughout the fourth shading scenario, the best success rate value of 98% is achieved by the SFS method followed by the CS optimizer (96%), while the worst rate value of 54% is assigned to the IWO and FPA optimizers. Out of 50 runs, as presented in Table A2, SFS failed only one time (run# 20) to reach the global power of 1129.4 W . IWO and FPA did not reach the global power 23 times. A summary of the evaluation of the statistical performance of different considered global MPPT methods is presented in Table 3. More details about the extracted power of each optimizer are shown in Table A2. The minimum standard deviation of 4.99 is achieved by SFS, followed by JAYA, whereas the largest value of 119.16 is assigned to the IWO optimizer. Correspondingly, the minimum RMSE of 5.16 is achieved by SFS. Overall, for the fourth shading scenario, the SFS optimizer accomplished the best performance compared with other methods.

Table 3. Statistical performance of different considered global MPPT methods.

	ALO	GSA	FPA	SFS	IWO	FA	CS	JAYA	ALO	GSA	FPA	SFS	IWO	FA	CS	JAYA
1. SR									2. Standard Deviation							
1st scenario	58	64	58	94	68	94	88	88	108.45	42.96	67.49	4.11	93.98	10.47	135.23	11.66
2nd scenario	60	90	80	100	80	96	90	100	32.92	25.68	28.56	0.09	24.02	3.93	19.22	0.01
3rd scenario	56	28	40	94	64	96	80	78	120.06	50.58	56.3	5.8	101	32.94	88.8	52.62
4th scenario	60	72	54	98	54	94	96	94	115.3	32.33	39.85	4.99	119.16	58.15	102.6	8.16
5th scenario	50	52	48	100	64	90	74	84	59.11	31.69	18.08	1.34	79.84	26.84	39.25	64.09
6th scenario	48	36	42	96	64	92	86	84	89.91	46.14	51.17	7.43	75.35	48.41	54.23	38.06
Average	55.33	57	53.67	97	65.67	93.67	85.67	88	87.63	38.23	43.58	3.96	82.22	30.12	73.22	29.1
3. Coefficient of Variation									4. Average (RE)							
1st scenario	0.117	0.045	0.071	0.004	0.099	0.011	0.144	0.012	6.16	2.48	3.2	0.14	4.12	0.25	5	0.43
2nd scenario	0.06	0.046	0.051	0.000	0.043	0.007	0.034	0.000	3.00	0.98	1.92	0.01	1.71	0.15	0.72	0.00
3rd scenario	0.096	0.039	0.044	0.004	0.079	0.025	0.069	0.04	6.17	3.53	3.28	0.23	4.82	0.46	3.29	1.53
4th scenario	0.109	0.029	0.036	0.004	0.114	0.053	0.093	0.007	5.29	1.66	2.22	0.12	6.55	1.07	1.73	0.18
5th scenario	0.063	0.033	0.019	0.001	0.084	0.027	0.041	0.066	4.79	2.4	1.72	0.05	4.19	0.9	2.33	1.89
6th scenario	0.071	0.036	0.04	0.006	0.059	0.037	0.041	0.029	5.65	3.05	3.3	0.2	3.84	1.03	1.55	0.93
Average	0.086	0.038	0.043	0.003	0.08	0.026	0.07	0.026	5.18	2.35	2.61	0.12	4.2	0.64	2.44	0.82
5. MAE									6. RMSE							
1st scenario	61.41	24.74	31.91	1.39	41.04	2.46	49.86	4.24	124.63	49.58	74.66	4.34	102.55	10.75	144.13	12.41
2nd scenario	29.87	9.79	19.14	0.05	17.06	1.5	7.18	0.01	37.1	26.28	30.6	0.09	25.93	4.02	19.65	0.01
3rd scenario	61.51	35.19	32.65	2.26	48.02	4.54	32.75	15.22	146.19	69.54	71.62	6.56	120.17	33.5	99.28	56.52
4th scenario	52.69	16.51	22.08	1.17	65.24	10.61	17.27	1.81	129.84	37.36	47.05	5.16	140.23	59.38	104.45	8.41
5th scenario	47.7	23.9	17.13	0.51	41.75	8.98	23.27	18.81	75.96	39.7	24.91	1.43	90.09	28.31	45.63	66.79
6th scenario	56.33	30.36	32.93	1.96	38.3	10.24	15.47	9.23	117.97	61.83	67.91	7.89	91.51	50.35	58.14	40.06
Average	51.59	23.42	25.97	1.22	41.9	6.39	24.3	8.22	105.28	47.38	52.79	4.24	95.08	31.05	78.55	30.7
7. Efficiency									8. Population Variance							
1st scenario	93.84	97.52	96.8	99.86	95.88	99.75	95	99.57	11,761.03	1845.6	4554.92	16.91	8831.84	109.63	18,288.5	135.96
2nd scenario	97	99.02	98.08	100	98.29	99.85	99.28	100	1083.58	659.32	815.9	0.01	576.73	15.45	369.42	0.000
3rd scenario	93.83	96.47	96.72	99.77	95.18	99.55	96.72	98.47	14,414.99	2557.98	3169.99	33.61	10,201.81	1084.86	7885.36	2768.9
4th scenario	94.71	98.34	97.78	99.88	93.45	98.94	98.27	99.82	13,293.3	1045.47	1587.75	24.89	14,199.52	3381.89	10,527.1	66.57
5th scenario	95.21	97.6	98.28	99.95	95.81	99.1	97.67	98.11	3494.47	1004.54	327.05	1.78	6374.1	720.63	1540.75	4107.84
6th scenario	94.35	96.95	96.7	99.8	96.16	98.97	98.45	99.07	8084.37	2128.54	2618.88	55.23	5677.65	2343.24	2941.08	1448.38
Average	94.82	97.65	97.39	99.88	95.8	99.36	97.56	99.18	8688.62	1540.24	2179.08	22.07	7643.61	1275.95	6925.37	1421.28

Table 3. Cont.

	ALO	GSA	FPA	SFS	IWO	FA	CS	JAYA	ALO	GSA	FPA	SFS	IWO	FA	CS	JAYA
9. Minimum value									10. Average value							
1st scenario	571.26	808.09	571.26	974.35	571.26	932.38	571.26	932.52	935.18	971.85	964.68	995.2	955.55	994.13	946.73	992.35
2nd scenario	407.84	387.22	438.11	570.78	450.69	545.01	438.81	571.22	554.14	565.65	560.29	571.23	561.49	570.41	567.15	571.26
3rd scenario	812.59	1145.18	1126.53	1324.41	987.56	1129.41	1129.41	1129.4	1268	1303.68	1307.13	1348.33	1286.3	1345.26	1307.01	1330.76
4th scenario	571.26	998.68	886.01	1095	571.26	755.25	456.99	1076.61	1069.7	1110.69	1104.38	1128.08	1055.48	1117.39	1109.85	1127.35
5th scenario	766.35	858.85	906.94	988.93	615.1	906.98	907.06	571.26	948.89	972.69	979.46	996.08	954.84	987.61	973.32	977.78
6th scenario	1024.74	1171.01	1199.44	1301.42	1129.41	1129.41	1129.41	1129.38	1275.03	1310.23	1306.75	1348.75	1299.48	1337.54	1330.44	1338.88
Average	692.34	894.84	854.72	1042.48	720.88	899.74	772.16	901.73	1008.49	1039.13	1037.11	1064.61	1018.86	1058.72	1039.08	1056.4

The fifth shading scenario is applied to the third PV configuration, where four series PV modules are connected in series. The solar irradiance levels distribution on the four PV modules are 1000 W/m^2 , 700 W/m^2 , 400 W/m^2 and 200 W/m^2 , respectively. Under this condition, there are four peaks: 571.3 W, 996.59 W, 907.1 W and 615.1 W. The global maximum power is located at the second left side of the power–voltage curve. The corresponding PV voltage and current at global power are 103.83 V and 9.60 A. The sixth shading scenario is also applied to the third PV configuration with varying the solar irradiance levels: 1000 W/m^2 , 800 W/m^2 , 600 W/m^2 and 400 W/m^2 , respectively. This variation leads to the transfer of the global power from the second left, to the second right side of the power–voltage curve. The peak power values of are 571.3 W, 1129.4 W, 1351.4 W and 1232 W. The global maximum power is located at the second left. The corresponding PV voltage and current at global power are 163.48 V and 8.27 A. More details about the performance of each optimizer under different shading scenarios can be found in Tables A1–A3.

As an example, the PV power variations throughout the optimization procedure using the SFS based tracker under the fourth and fifth shading scenarios, are presented in Figures 6 and A1, respectively. Considering Figure 6, it is confirmed that during the fifth shading scenario, out of 50 runs, the SFS based tracker failed to reach the target maximum power only one time. At run#20, the extracted maximum power is 1095 W. This means the efficiency under this situation is 96.86%. The decision variable (duty cycle) variations during the optimization process of the SFS based tracker (a) forth shading scenario (b) fifth shading scenario, are illustrated in Figure 7. It can be noted that all particles converge to the optimal solution.

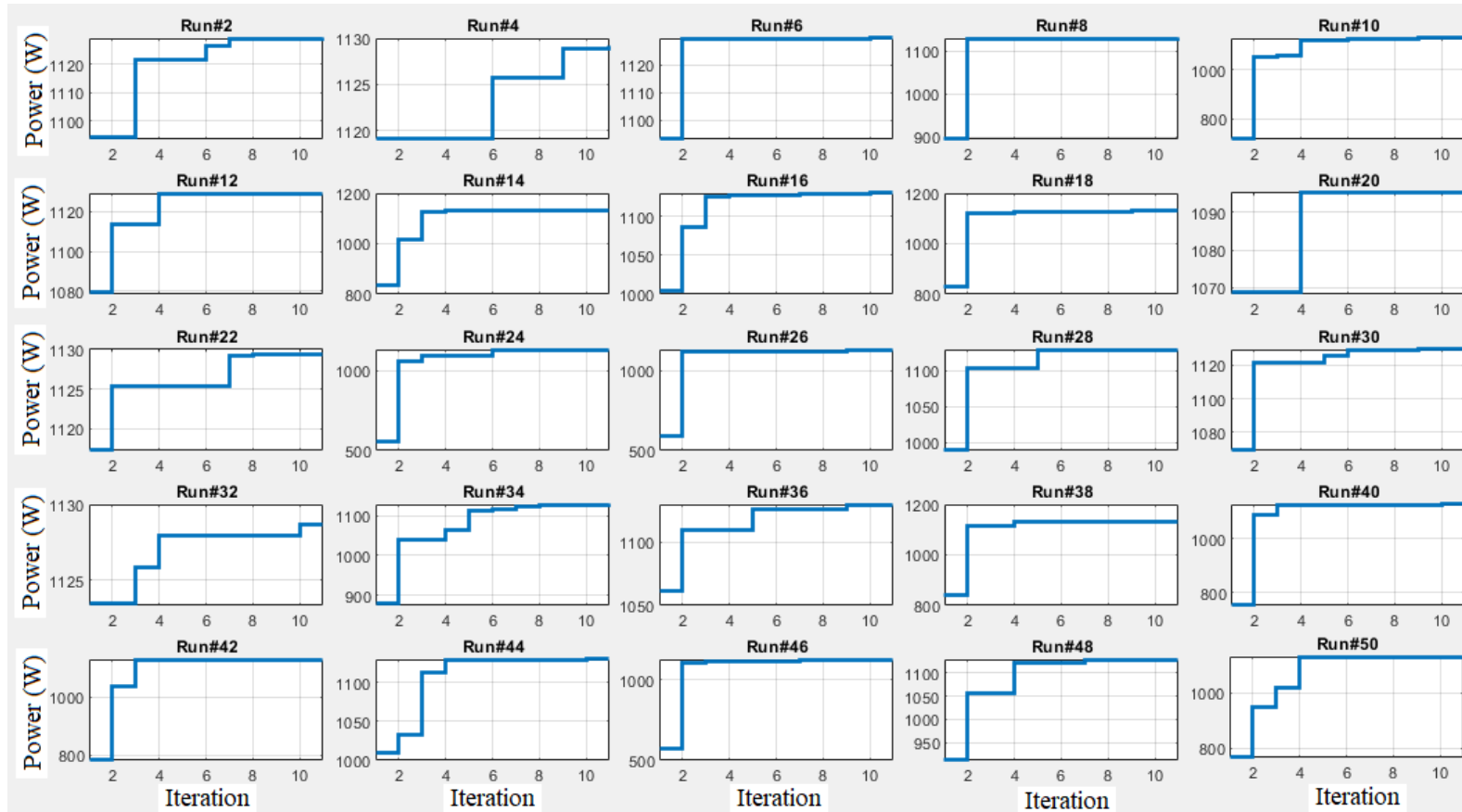


Figure 6. The PV power variation during optimization process using SFS based tracker under fourth shading scenario.

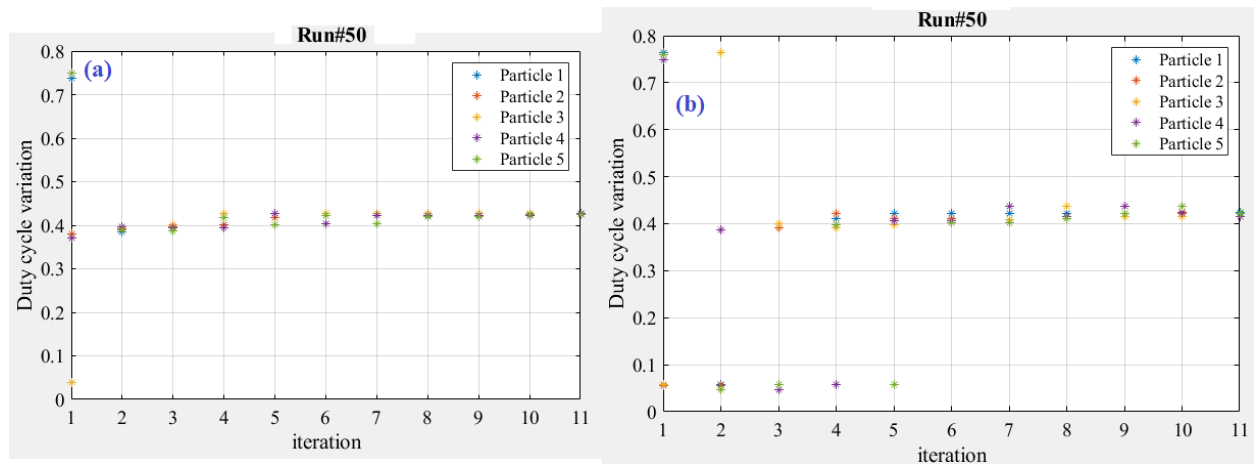


Figure 7. Decision variable (duty cycle) variation during optimization process of SFS based tracker (a) fourth shading scenario (b) fifth shading scenario.

Table 4 and Figure 8 present a comprehensive performance comparison among different, considered global, MPPT methods. They summarize the average values for different evaluation metrics during six shading scenarios. It can be concluded that the best optimizer is SFS. It achieved the best values for different performance evaluation metrics. For the success rate, the optimizers are ranked as follows: SFS, FA, JAYA, CS, IWO, GSA, ALO and FPA. The tracking efficiency for all optimizers is greater than 94%. The maximum value of 99.88% is achieved by SFS, followed by FPA and JAYA, whereas the minimum value of 94.8% is assigned to ALO. The average minimum RSME is 7.89 that is achieved by SFS. The worst RMSE of 117.97 is assigned to ALO. Ranking of the considered global MPPT methods is illustrated in Table 5 and its radar plot is presented in Figure 9. It can be finally concluded that SFS has superior performance compared with other methods, followed by FA, JAYA, GSA, CS, FPA, IWO and ALO.

Table 4. A comparison among considered algorithms.

Optimizer	ALO	GSA	FPA	SFS	IWO	FA	CS	JAYA
SR	55.33	57.00	53.67	97.00	65.67	93.67	85.67	88.00
StD	87.63	38.23	43.58	3.96	82.22	30.12	73.22	29.10
Coefficient of Variation	0.091	0.04	0.04	0.003	0.08	0.03	0.07	0.03
Average (RE)	5.18	2.35	2.61	0.12	4.20	0.64.00	2.44	0.82
MAE	51.59	23.42	25.97	1.22	41.90	6.39	24.30	8.22
RMSE	117.97	61.83	67.91	7.89	91.51	50.35	58.14	40.06
Efficiency	94.82	97.65	97.39	99.88	95.80	99.36	97.56	99.18
Variance	8688.62	1540.24	2179.08	22.07	7643.61	1275.95	6925.37	1421.28
Minim value	692.34	894.84	854.72	1042.48	720.88	899.74	772.16	901.73
Average value	1008.49	1039.13	1037.11	1064.61	1018.86	1058.72	1039.08	1056.4

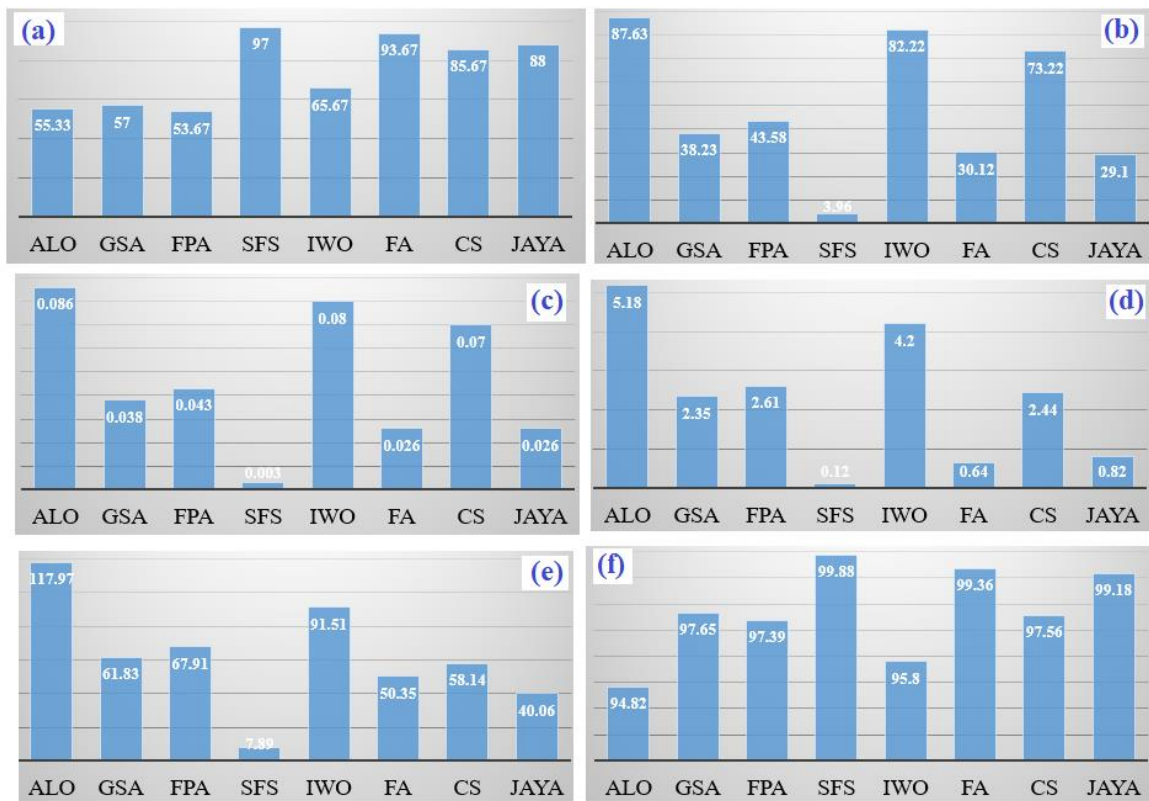


Figure 8. Performance comparison of different considered optimizers (a) success rate (SR); (b) standard deviation (StD); (c) coefficient of variation; (d) Average (RE); (e) RMSE and (f) Efficiency.

Table 5. Ranking of considered global MPPT methods.

Optimizer	ALO	GSA	FPA	SFS	IWO	FA	CS	JAYA
SR	7	6	8	1	5	2	4	3
StD	8	4	5	1	7	3	6	2
Coefficient of Variation	8	6	7	1	3	4	2	4
Average (RE)	8	4	6	1	7	2	5	3
MAE	8	4	6	1	7	2	5	3
RMSE	8	5	6	1	7	3	4	2
Efficiency	8	4	6	1	7	2	5	3
Variance	8	4	5	1	7	2	6	3
Minim value	8	4	5	1	7	3	6	2
Average value	8	4	6	1	7	2	5	3
Overall Rank	8	4	6	1	7	2	5	3

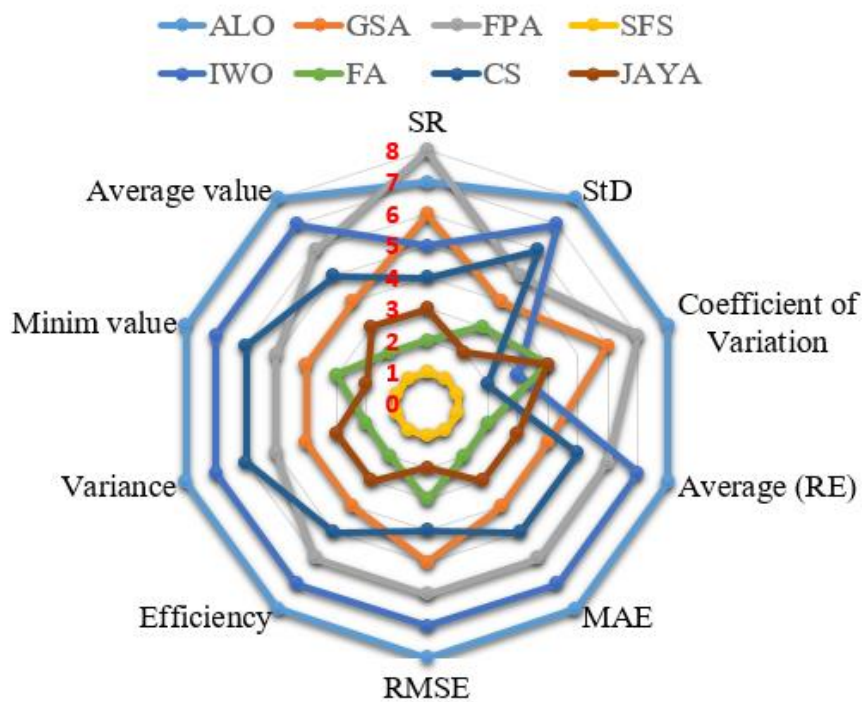


Figure 9. Radar plot for ranking considered global MPPT methods.

5. Conclusions

In this paper, for the first time, a stochastic fractal search (SFS) optimization algorithm is used to extract the global power of the PV system employing triple-junction solar cells under shading conditions. To prove and test the reliability of SFS optimizer, different evaluation metrics are considered: success rate (SR), standard deviation (StD), coefficient of variation, average relative error (RE), mean absolute error (MAE), root mean square error (RMSE), efficiency, population variance, minima value, and average value. Three PV configurations: two modules in series, three modules in series, and four models in series are used in the evaluation process. For every configuration, two different shading scenarios are used. The idea of changing the shading scenario is to change the position of the global MPP. The obtained results are compared with common optimizers: the Antlion Optimizer (ALO), Cuckoo Search (CS), Flower Pollination Algorithm (FPA), Firefly-Algorithm (FA), Invasive-Weed-Optimization (IWO), JAYA and Gravitational Search Algorithm (GSA). SFS achieved the best values for different performance evaluation metrics. For the success rate, the optimizers are ranked as follows: SFS, FA, JAYA, CS, IWO, GSA, ALO and FPA. The tracking efficiency for all optimizer is greater than 94%. The maximum value of 99.88% is achieved by SFS, followed by FPA and JAYA, whereas the minimum value of 94.8% is assigned to ALO. The average minimum RSME is 7.89 that achieved by SFS. The worst RMSE of 117.97 is assigned to ALO. In sum, it can be concluded that SFS has superior performance compared with the other methods, followed by FA, JAYA, GSA, CS, FPA, IWO and ALO.

Author Contributions: Conceptualization, H.R. and A.F.; formal analysis, H.R. and A.F.; investigation, H.R.; methodology, H.R. and A.F.; software, H.R.; writing—original draft, H.R. and A.F.; writing—review & editing, H.R. and A.F. All authors have read and agreed to the published version of the manuscript.

Funding: This project was supported by the Deanship of Scientific Research at Prince Sattam Bin Abdulaziz University under the research project No. 2020/01/11742.

Conflicts of Interest: The authors declare no conflict of interest.

Abbreviations and Acronyms

MPPT	maximum power point tracking
SFS	stochastic fractal search
PV	photovoltaic
ALO	Antlion Optimizer
CS	Cuckoo Search
FPA	Flower Pollination Algorithm
FA	firefly-algorithm
IWO	invasive-weed-optimization
GSA	Gravitational Search Algorithm
CPVS	Concentrating PV System
P&O	perturb and observe
INC	incremental conductance
SR	success rate
StD	standard deviation
RE	average relative error
MAE	mean absolute error
RMSE	root mean square error

Symbols

T_{Ref}	reference temperature in °C
a	short circuit current temperature coefficient in A/°C
K_C	concentration ratio, and G is the solar radiation in W/m ²
q	electron charge
n_i	diode ideality factor
K_B	Boltzmann's constant
E_g	bandgap energy
K	constant
γ	constant
T	absolute temperature,
R_S	cell series resistance
E_i	energy of particle
E	the maximum considered potential energy
P	number of particles
U_b	the search space upper bound
L_b	the search space lower bound
g	the number of iterations
ψ	fixed value of 1.5.

Appendix A

Table A1. The detailed performance of each optimizer for the 1st and 2nd shading scenarios.

Run	1st Shading Scenario							2nd Shading Scenario								
	ALO	GSA	FPA	SFS	IWO	FA	CS	JAYA	ALO	GSA	FPA	SFS	IWO	FA	CS	JAYA
1	996.59	994.3	930.48	996.58	996.59	996.59	571.26	996.59	493.62	570.99	569.82	571.26	571.26	571.26	571.26	571.26
2	996.53	996.35	995.45	996.57	798.98	996.59	996.59	995.04	571.26	571.08	570.37	571.26	571.26	571.26	564.11	571.26
3	764.04	996.56	994.6	996.53	976.03	996.59	996.59	963.42	565.51	555.72	571.06	571.25	571.26	571.26	571.26	571.26
4	934.49	990.61	995.78	991.03	856.53	996.59	996.59	995.79	503.1	569.93	570.22	571.26	565.32	571.26	551.86	571.26
5	995.56	983.05	980.59	996.53	911.69	996.59	996.59	996.57	571.26	566.04	570.97	571.26	571.26	571.26	571.26	571.26
6	953.66	827.47	996.58	996.53	996.59	996.59	996.59	995.8	537.89	571.25	569.66	571.26	571.26	571.26	571.26	571.25
7	996.59	996.37	970.11	996.43	933.22	996.59	996.59	996.51	571.26	570.45	438.8	571.25	571.26	571.26	571.26	571.23
8	843.77	987.34	996.24	996.27	996.59	996.59	996.59	996.59	571.15	568.76	570.68	571.22	543.93	545.01	571.26	571.26
9	571.26	921.56	995.69	996.58	996.59	964.65	996.59	989.35	535.23	566.62	546.47	571.21	568.88	571.26	571.26	571.24
10	828.25	996.14	859.08	996.59	967.18	996.59	996.59	996.56	570.76	570.66	561.72	571.26	571.26	571.26	571.26	571.26
11	750.24	996.52	990.51	996.51	996.59	996.59	571.26	996.46	535.52	571	438.11	571.17	544.54	571.26	571.26	571.26
12	996.59	996.55	982.14	996.54	996.59	996.59	996.59	995.57	521.6	567.86	571.26	571.26	571.26	566.04	571.26	571.26
13	992.21	988.25	990.32	996.58	996.59	996.59	996.59	996.58	567.24	571.25	571.13	571.25	570.87	571.26	571.26	571.26
14	966.79	984.5	963.53	996.57	571.26	996.59	996.59	995.33	565.19	387.22	571.23	571.22	571.26	571.26	571.26	571.26
15	991.91	994.46	957.74	996.07	996.59	996.59	996.59	996.57	555.96	571.15	515.37	571.17	571.26	571.26	571.26	571.26
16	909.73	996.11	891.53	996.51	966.76	996.58	630.22	996.51	554.33	570.64	571.02	571.26	571.26	571.26	535.23	571.26
17	906.55	995.59	995.97	996.48	996.59	996.59	996.59	996.38	570.95	571.16	571.15	571.22	503.07	571.26	571.26	571.25
18	996.44	921.87	995.92	996.58	816.95	996.59	996.59	996.59	571.26	571.15	571.26	571.26	547.4	571.26	571.26	571.26
19	995.4	959.64	989.02	996.34	996.59	996.59	996.59	957.67	571.26	571.26	571.05	571.26	571.26	571.26	571.26	571.26
20	996.59	996.45	996.17	996.04	996.59	996.59	996.59	996.56	571.26	570.36	571.24	571.26	571.26	571.26	571.26	571.26
21	996.56	994.83	934.32	994.23	996.59	996.59	996.59	996.58	570.86	571.26	571.26	570.9	571.26	571.26	571.26	571.24
22	996.59	996.33	993.2	996.57	996.59	996.59	996.59	996.07	407.84	569.72	567.59	571.26	571.26	571.26	571.26	571.26
23	871.27	995.26	996.36	996.59	996.59	996.59	996.59	996.56	571.17	569.04	570.82	571.26	450.69	571.26	571.26	571.26
24	992.79	986.15	995.25	982.72	996.59	996.59	996.59	996.54	555.16	570.03	571.22	571.26	570.44	571.26	571.26	571.22
25	996.24	808.09	988.37	996.49	996.59	996.59	996.59	996.59	528.36	569.83	571.26	571.25	571.26	571.26	571.26	571.26
26	996.59	996.36	995.77	996.52	996.59	996.59	996.59	996.59	551.27	569.14	571.22	571.26	571.26	571.26	571.26	571.26
27	996.59	995.33	995.38	996.59	996.59	996.59	996.58	996.59	571.26	565.57	555.2	571.25	571.26	571.26	571.26	571.26

Table A1. Cont.

Run	1st Shading Scenario								2nd Shading Scenario							
	ALO	GSA	FPA	SFS	IWO	FA	CS	JAYA	ALO	GSA	FPA	SFS	IWO	FA	CS	JAYA
28	980.53	987.88	996.56	996.58	995.05	932.38	996.59	996.59	438.81	571.23	570.35	571.26	567.3	571.26	571.26	571.26
29	886.81	951.43	942.48	996.59	996.59	996.58	996.59	996.56	537.29	567.45	569.02	571.23	532.48	571.26	571.26	571.25
30	961.41	996.42	994.65	995.45	996.59	996.59	996.59	996.59	564.53	571.24	571.21	571.26	537.91	571.26	571.26	571.26
31	996.59	996.56	957.84	995.69	782.4	995.31	996.59	996.59	571.26	568.63	571.26	571.26	571.26	571.26	568.29	571.26
32	996.59	995.32	571.26	996.59	996.59	996.59	996.59	996.59	571.26	570.87	570.5	571.26	571.26	571.26	569.55	571.26
33	996.33	996.31	970.67	995.71	996.59	996.59	996.59	996.59	571.26	570.83	570.18	571.26	571.26	571.26	571.26	571.26
34	996.59	945.51	979.82	996.54	996.59	996.59	996.59	995.99	518.3	562.77	568.48	571.25	571.26	571.26	571.26	571.26
35	978.27	996.17	955.64	996.57	996.59	996.59	571.26	996.54	571.26	571.26	561.39	571.26	571.26	571.26	571.26	571.26
36	996.59	996.19	839.03	996.03	952.78	996.59	996.59	996.58	571.26	569.61	571	571.26	571.26	561.75	571.26	571.26
37	989.51	883.8	993.14	996.59	571.26	996.59	996.58	991.36	571.26	570.6	570.5	571.25	571.26	571.26	571.26	571.26
38	996.59	996.51	994.31	995.87	996.59	996.59	996.59	985.47	571.26	571.26	570.78	571.26	571.26	570.07	571.26	571.26
39	996.59	992.17	993.11	996.55	996.59	996.58	571.26	994.57	571.26	571.25	571.26	571.26	571.26	571.26	565.34	571.26
40	996.59	996.46	985.25	996.55	961.31	996.58	996.59	993.7	571.26	570.01	531.45	571.26	571.26	571.26	571.26	571.26
41	990.34	984.36	867.5	982.12	996.47	996.59	996.59	996.51	561.66	560.4	571.26	571.26	571.26	571.26	571.26	571.26
42	996.59	892.7	996.54	996.5	933.26	971.32	996.58	996.41	569.6	570.69	570.92	571.26	571.26	571.26	571.26	571.26
43	907.92	953.01	925.08	996.35	996.59	996.59	996.59	996.59	571.15	571.25	566.59	571.26	571.26	571.26	571.26	571.26
44	651.08	971	988.92	974.35	978.38	996.59	996.59	996.59	571.26	570.01	566.7	571.26	517.17	571.26	571.26	571.26
45	742.15	952.68	968.23	995.33	996.59	996.59	996.59	981.63	568.43	571.12	570.31	570.78	571.26	571.26	571.26	571.26
46	996.59	910.04	967.11	995.16	996.48	996.59	996.58	932.52	571.26	571.16	570.8	571.26	571.26	571.26	571.26	571.26
47	996.59	925.24	996.55	995.57	917.46	996.59	996.58	994.69	571.26	563.25	571.23	571.18	571.26	570.7	571.26	571.26
48	571.26	995.87	996.22	996.57	996.59	996.59	571.26	996.59	548.02	571.26	499.77	571.2	488.81	571.26	438.81	571.26
49	973.04	995.56	991.9	996.57	996.59	996.59	996.59	996.55	571.26	566.02	547.25	571.2	571.26	571.26	571.26	571.26
50	934.86	989.16	995.91	996.59	996.59	996.59	996.59	973.61	571.26	571.19	571.09	571.26	571.26	571.26	571.26	571.26

Table A2. The detailed performance of each optimizer for the 3rd and 4th shading scenarios.

Run	3rd Shading Scenario								4th Shading Scenario							
	ALO	GSA	FPA	SFS	IWO	FA	CS	JAYA	ALO	GSA	FPA	SFS	IWO	FA	CS	JAYA
1	1351.42	1307.49	1261.59	1351.4	1290.65	1351.37	1129.41	1351.42	1129.41	1127.61	1116.32	1129.41	984.62	1129.41	1129.41	1076.61
2	1193.59	1320.68	1133.97	1347.46	1351.42	1351.42	1129.41	1350.54	1129.3	1128.3	1064	1129.3	1129.41	1129.41	1129.41	1129.41
3	1350.08	1321.68	1285.9	1350.03	1351.42	1351.39	1351.42	1342.21	1092.04	998.68	1119.9	1129.4	1129.41	1129.41	1129.41	1107.97
4	1351.42	1351.23	1346.38	1349.88	1351.42	1351.42	1129.41	1348.92	1111.61	1125	1127.75	1129.21	571.26	1129.41	1129.41	1129.41
5	1112.64	1351.24	1351.02	1351.38	1351.42	1351.41	1351.41	1350.51	1129.41	1071.02	1129.29	1128.82	1129.41	1129.41	1129.41	1129.39
6	1305.31	1351.08	1248.22	1351.04	1351.42	1351.06	1351.42	1331.93	1129.41	1106.51	1094.83	1129.41	1129.41	1129.41	1129.41	1129.33
7	1129.41	1351.41	1298.65	1351.4	987.56	1351.42	1351.42	1351.37	1003.2	1126.38	1078.5	1129.39	1129.41	1129.41	1129.41	1129.41
8	1235.56	1326.85	1349.98	1342.92	1129.41	1351.42	1129.41	1348.87	571.26	1126.81	1087.75	1129.4	1096.43	1129.41	1129.41	1129.4
9	1351.42	1346.66	1319.55	1351.26	1351.42	1351.36	1351.42	1351.41	1129.41	1124.49	1121.48	1129.41	1010.61	1129.41	1129.41	1129.4
10	812.59	1350.85	1258.75	1351.17	1351.42	1351.41	1351.4	1129.41	1129.24	1129.41	1125.06	1129.39	973.49	1129.41	1129.41	1129.41
11	1351.42	1349.08	1333.59	1351.37	1129.41	1351.41	1351.41	1334.34	1056.59	1129.38	1102.32	1127.98	1070.83	1129.41	1129.41	1129.12
12	1351.42	1318.32	1332	1351.41	1314.22	1351.39	1129.41	1351.41	1129.41	1050.08	886.01	1129.18	1129.41	1129.41	1129.41	1129.41
13	1129.41	1351.36	1342.63	1326.58	1129.41	1351.42	1351.39	1351.41	998.4	1099.9	1127.79	1129.34	1129.41	1129.41	823.92	1129.17
14	1351.41	1241.38	1335.35	1351.37	1351.42	1351.38	1351.41	1349.46	1129.41	1036.49	1125.74	1129.37	1129.41	1129.41	1129.41	1129.36
15	1351.42	1277.46	1351.41	1346.66	1351.42	1351.42	1351.42	1351.41	1129.41	1129.28	1090.51	1129.41	1129.41	1129.41	1129.41	1129.41
16	1117.59	1348.94	1326.24	1351.36	1351.42	1351.4	1351.41	1350.75	922.54	1119.35	1128.05	1129.41	1062.02	1129.41	1129.41	1129.37
17	1351.42	1288.36	1348.92	1351.37	1129.41	1351.32	1351.42	1351.12	1129.41	1121.76	1117.38	1129.41	1129.41	1129.41	1129.41	1129.41
18	1129.41	1315.63	1237.32	1351.41	1129.41	1351.42	1351.42	1312.69	1129.25	1066.6	1128	1129.41	810.94	1129.41	1129.4	1129.31
19	1351.19	1328.89	1332.01	1341.65	1351.42	1351.42	1351.41	1350.47	1102.11	1126.62	1123.76	1122.96	1129.41	1129.41	1129.41	1129.41
20	1129.23	1257	1297.06	1350.86	1129.41	1351.41	1351.42	1351.38	1007.31	1128.94	1129.36	1095	1081.3	1129.41	1129.41	1129.41
21	1322.02	1299.09	1347.6	1345.82	1351.42	1351.41	1129.41	1129.41	1129.41	1129.41	1096.19	1120.3	871.91	1129.41	1129.41	1129.41
22	1351.42	1321.74	1327.89	1351.41	1129.41	1351.41	1351.42	1347.97	1103.19	1096.97	1082.72	1129.4	1129.41	1129.4	1129.41	1129.05
23	1350.14	1344.51	1351.36	1351.35	1129.41	1351.36	1351.42	1347.37	1129.41	1129.09	1066.06	1127.58	858.92	1088.79	1129.41	1129.41
24	1351.42	1301.94	1319.74	1349.51	1351.42	1351.42	1351.41	1302.43	800.95	1119.95	1127.47	1129.32	1129.41	1129.41	1129.41	1129.41
25	1317.21	1216.37	1311.53	1351.08	1351.42	1351.41	1351.38	1129.4	1129.24	1129.08	1116.5	1128.41	1129.41	1129.41	1129.41	1121.23
26	1129.41	1315.47	1256.1	1335.3	1351.42	1351.42	1351.41	1351.31	1129.41	1125.3	1061.94	1129.32	1047.7	1129.4	1129.41	1129.4
27	1351.42	1317.78	1126.53	1324.41	1351.42	1349.58	1351.42	1351.02	1129.3	1127.58	1121.41	1129.39	1129.41	943.2	1129.41	1129.41
28	1351.42	1349.2	1300.28	1349.9	1351.42	1351.42	1351.4	1343.35	749.76	1077.13	1101.87	1129.32	1089.73	1129.41	1129.41	1129.41
29	1129.41	1328.87	1349.7	1351.07	1351.42	1351.41	1351.41	1351.34	1077.88	1129.01	1129.02	1129.4	982.52	1129.39	1129.41	1129.41
30	1273.17	1331.99	1344.89	1349.37	1351.42	1129.41	1351.38	1289.7	1129.41	1127.85	1129.28	1129.41	1129.41	1129.41	1129.41	1129.38

Table A2. Cont.

Run	3rd Shading Scenario								4th Shading Scenario							
	ALO	GSA	FPA	SFS	IWO	FA	CS	JAYA	ALO	GSA	FPA	SFS	IWO	FA	CS	JAYA
31	1276.8	1303.6	1350.41	1351.42	1129.41	1351.41	1351.41	1351.16	1128.19	1129.07	1094.03	1129.41	946.07	1129.41	1129.41	1129.37
32	1351.24	1351.41	1345.65	1345.3	1351.41	1268.67	1351.42	1307.63	1129.41	1129.18	1107.59	1128.7	933.17	1129.41	1129.41	1127.81
33	1347.79	1351.42	1336.77	1351.03	1171.71	1351.41	1351.42	1349.36	1024.49	1128.33	1129.24	1128.68	1129.41	1129.41	1129.41	1129.4
34	1129.41	1350.11	1336.12	1343.53	1351.41	1351.4	1351.41	1339.34	1129.27	1117.03	1129.41	1129.27	1095.82	1129.41	1129.41	1128.97
35	1350.36	1145.18	1234.84	1351.11	1351.42	1351.41	1351.42	1351.3	1129.41	1124.11	1123.52	1128.78	1129.41	1129.41	1129.41	1128.1
36	1338.01	1187.94	1241.96	1350.38	1351.42	1351.42	1351.42	1344.86	1129.41	1129.41	1057.09	1129.41	1104.2	1129.41	1129.41	1129.4
37	1351.42	1227.55	1161.49	1351.16	1351.42	1351.34	1351.42	1351.07	1129.4	1128.53	1129.05	1126.42	1129.41	1129.41	1129.41	1129.31
38	1351.42	1323.14	1351.29	1351.4	1129.41	1351.42	1351.41	1329.16	1101.91	1091.09	1129.3	1129.41	1129.41	1129.41	1129.41	1114.56
39	1351.33	1262.18	1328.17	1351.42	1300.4	1351.31	1129.41	1331.94	845.76	1125.1	1129.19	1128.11	1129.41	1129.41	1129.41	1129.41
40	1079.36	1217.94	1237.77	1348.59	1351.42	1351.42	1351.42	1343.43	875.66	1118.94	1124.1	1129.41	729.24	1129.41	1129.41	1129.41
41	1351.42	1303.94	1350.65	1351.41	1279.71	1351.41	1129.41	1338.54	1129.41	1129.19	1053.49	1129.37	1129.41	1129.41	1129.41	1129.41
42	1351.4	1331.21	1242.02	1346.4	1351.42	1351.41	1351.42	1346.44	1129.41	1126.79	1129.23	1129.41	1129.41	1129.41	1129.41	1128.99
43	1188.72	1337.84	1351.15	1350.45	1351.42	1351.42	1351.42	1351.42	1077.42	1110.95	1049.5	1129.4	1012.23	1129.41	1129.41	1129.41
44	979.57	1179.29	1345.61	1348.01	1351.42	1351.41	1351.4	1351.42	998.58	1037.38	1052	1129.31	1129.41	1129.41	1129.41	1129.41
45	1351.41	1265.6	1333.71	1351	1301.83	1351.36	1351.4	1350.91	1120.12	1122.66	1126.03	1127.33	1087.47	1129.41	1129.41	1129.04
46	1233.74	1266.76	1350.43	1351.16	1129.41	1351.42	1129.41	1351.4	1129.41	1128.94	1125.66	1129.26	1129.41	1129.41	1129.41	1129.41
47	1351.42	1322.44	1348.42	1350.46	1351.42	1351.4	1351.42	1341.63	1123.81	1126.5	1129.23	1129.1	1129.41	1129.41	1129.41	1129.41
48	1349.55	1334.55	1304.97	1351.41	1351.42	1351.42	1351.42	1351.41	1129.4	1010.06	1113.27	1129.41	906.21	1129.41	1129.41	1129.4
49	1350.54	1296.76	1340.13	1339.2	1351.42	1351.42	1129.41	1349.88	1129.41	1128.86	1105.13	1128.53	953.5	1129.4	456.99	1129.4
50	1230.65	1242.62	1338.85	1350.71	1351.42	1351.35	1351.41	1351.42	1099.05	1128.43	1126.45	1129.01	1128.88	755.25	1129.41	1129.41

Table A3. The detailed performance of each optimizer for the 5th and 6th shading scenarios.

Run	5th Shading Scenario								6th Shading Scenario							
	ALO	GSA	FPA	SFS	IWO	FA	CS	JAYA	ALO	GSA	FPA	SFS	IWO	FA	CS	JAYA
1	939.38	950.51	990.08	995.98	907.11	996.59	996.59	996.55	1351.42	1336.92	1348.42	1343.8	1351.42	1351.41	1339.96	1351.42
2	996.59	994.74	981.81	994.76	996.59	996.59	996.59	995.48	1351.42	1350.78	1199.44	1351.39	1129.41	1232.81	1351.41	1351.41
3	939.28	988.01	973.6	996.59	907.11	996.59	907.1	996.58	1129.41	1349.07	1305	1351.04	1351.42	1351.42	1351.41	1351.11
4	844.73	926.31	978.06	996.45	996.59	996.59	996.59	995.13	1319.3	1318.03	1303.07	1351.32	1351.42	1351.42	1351.41	1351.38
5	996.59	978.87	983.29	996.23	996.59	996.57	996.59	980.06	1209.81	1331.44	1224.09	1350.98	1232.81	1351.32	1351.42	1351.4
6	996.58	927.99	987.18	996.58	996.59	996.58	996.59	996.55	1350.36	1171.01	1347.6	1348	1351.42	1351.41	1351.42	1351.4
7	909.69	994.74	964.39	996.55	615.1	907.1	907.11	996.57	1232.81	1348.37	1205.61	1351.41	1351.42	1351.41	1351.41	1349.54
8	995.36	984.35	962.82	995.86	996.59	996.59	907.11	996.55	1351.42	1231.64	1351.04	1351.38	1232.81	1343.09	1351.41	1350.67
9	967.36	974.98	990.46	996.46	996.59	996.59	996.59	996.36	1351.41	1338.18	1349.93	1351.18	1351.42	1351.41	1351.4	1351.41
10	906.96	978.72	995.61	996.59	996.59	996.59	996.56	996.59	1351.41	1349.75	1350.45	1351.37	1351.42	1351.41	1351.42	1351.35
11	954.93	995.8	961.44	996.55	996.59	996.59	996.59	996.54	1223.46	1240.9	1351.01	1351.41	1129.41	1351.41	1351.41	1351.28
12	996.59	913.79	995.88	996.56	996.59	996.59	996.59	996.59	1203.42	1232.59	1200.91	1351.41	1351.42	1347.67	1351.36	1349.58
13	996.58	994.53	966.39	995.86	996.59	996.59	996.59	994.18	1351.42	1326.31	1351	1351.04	1351.42	1351.42	1351.42	1351.41
14	996.59	996.38	973.52	996.57	968.48	996.59	996.59	996.37	1351.42	1301.86	1228.04	1351.3	1232.81	1232.81	1351.42	1349.01
15	907.11	993.24	979.35	996.57	996.59	996.59	996.59	986.17	1351.42	1216.2	1281	1351.33	1351.42	1351.41	1351.41	1333.17
16	996.59	906.8	991.89	996.37	996.59	907.11	996.58	993.34	1213.4	1309.47	1337.02	1351.39	1351.42	1351.41	1351.42	1342.97
17	864.78	982.63	984.35	991.56	996.59	996.59	996.59	996.03	1349.12	1350.48	1350.88	1351.42	1351.42	1351.42	1351.42	1347.65
18	983.83	994.55	990.8	996.54	615.1	996.59	996.59	996.56	1232.81	1350.75	1350.64	1351.08	1129.41	1351.4	1232.79	1344.08
19	907.1	996.39	994.57	996.59	907.11	996.58	996.59	996.44	1114.19	1351.03	1326.12	1351.42	1351.42	1351.41	1351.42	1351.32
20	766.35	858.85	985.61	996.59	996.59	996.59	996.59	996.01	1351.42	1343.99	1312.09	1350.85	1351.42	1351.42	1129.41	1329.21
21	784.12	936.68	996.54	996.59	996.59	996.54	907.11	996.58	1351.41	1240.25	1346.05	1351.02	1351.42	1351.42	1351.39	1338.16
22	996.59	996.36	906.94	996.55	907.11	996.59	996.59	996.58	1301.8	1330.12	1345.14	1301.42	1351.42	1351.42	1351.41	1351.32
23	902.6	991.62	960.23	996.58	996.59	996.59	907.1	995.62	1232.81	1324.78	1249.8	1347.58	1351.42	1129.41	1351.42	1351.31
24	996.59	988.57	991.98	996.48	953.19	996.59	996.59	996.59	1338.74	1224.51	1227.18	1348.95	1232.81	1351.29	1351.41	1347.67
25	996.59	989.31	996.13	996.55	996.59	996.59	996.59	990.3	1128.36	1351.23	1232.66	1351.41	1348.39	1351.42	1351.41	1351.4
26	996.59	941.08	963.75	996.54	907.11	996.59	996.59	996.44	1105.75	1310.2	1350.39	1351.35	1232.81	1351.31	1351.42	1351.4
27	996.59	996.47	939.96	996.59	996.59	907.1	996.59	994.07	1351.42	1350.47	1351.37	1351.39	1351.42	1351.41	1351.42	1351.41
28	924.74	989.82	990.55	996.56	907.11	996.58	907.09	889.85	1350.96	1329.27	1350.68	1351.38	1232.81	1351.35	1232.81	1335.18
29	996.59	982.86	994.68	996.59	996.59	996.59	996.59	996.53	1351.41	1349.8	1346.01	1351.16	1351.42	1129.41	1351.42	1337.29
30	907.11	983.31	990.24	995.94	996.59	996.59	996.59	995.52	1351.32	1349.57	1332.32	1351.42	1129.41	1351.41	1351.42	1351.08
31	996.58	995.5	980.56	996.59	907.11	996.58	996.59	996.2	1232.81	1331.7	1335.1	1347.76	1232.81	1351.39	1351.41	1323.23
32	960.86	981.25	963.64	996.22	996.59	996.59	996.59	571.26	1232.81	1281.59	1323.51	1347.51	1351.42	1351.42	1351.41	1350.09

Table A3. Cont.

Run	5th Shading Scenario								6th Shading Scenario							
	ALO	GSA	FPA	SFS	IWO	FA	CS	JAYA	ALO	GSA	FPA	SFS	IWO	FA	CS	JAYA
33	907.11	996.44	993.84	996.59	996.59	996.59	996.59	986.99	1351.36	1300.8	1336.93	1342.73	1129.41	1351.41	1351.41	1351.41
34	885.45	938.28	990.12	996.44	996.59	996.54	996.59	902.57	1351.42	1223.62	1231.32	1350.45	1351.42	1351.42	1351.41	1349.11
35	866.26	905.37	996.55	995.83	996.59	996.59	907.1	996.59	1024.74	1334.06	1330.94	1350.91	1232.81	1351.42	1129.41	1349.27
36	926.53	996.42	979.84	996.59	907.11	996.55	907.11	996.36	1232.43	1335.73	1208.43	1351.41	1351.42	1351.42	1351.41	1350.39
37	996.59	996.58	995.78	996.28	996.59	996.59	996.59	907.05	1351.42	1327.92	1349.17	1345.87	1232.81	1351.42	1351.42	1342.39
38	996.59	996.22	963.32	996.48	996.59	996.59	996.59	958.68	1351.42	1287.83	1324.33	1345.1	1292.17	1351.4	1351.41	1349.15
39	996.59	996.49	961.18	993.35	907.11	996.59	907.1	996.59	1351.41	1292.35	1339.31	1351.19	1351.42	1351.41	1351.42	1351.41
40	996.59	986.92	996.44	988.93	996.59	995.58	907.1	987.75	1337.47	1341.78	1254.11	1351.16	1351.42	1351.41	1351.42	1351.42
41	996.59	911.19	989.76	996.58	996.59	996.59	996.59	887.88	1129.41	1298	1274.52	1351.41	1232.81	1351.42	1351.41	1351.16
42	907.11	983.36	985.93	996.19	907.11	996.53	907.1	996.59	1232.81	1351.37	1280.14	1345.29	1351.42	1351.42	1351.42	1351.38
43	992.82	971.77	995.25	996.59	907.11	996.59	996.59	995.88	1351.4	1299.38	1351.42	1351.4	1351.42	1351.42	1351.42	1351.37
44	996.59	972.83	993.1	996.56	907.11	907.1	996.59	996.59	1251.52	1351.35	1340.51	1349.03	1351.42	1351.41	1351.41	1231.64
45	996.44	965.42	948.62	996.59	996.59	996.59	996.59	995.47	1232.81	1291.23	1345.08	1336.01	1351.42	1351.41	1232.81	1349.7
46	857.23	946.23	956.01	995.61	996.59	996.59	907.06	996.59	1351.42	1350.83	1275.63	1351.42	1232.81	1351.42	1232.8	1351.41
47	996.59	986.65	996.59	996.59	996.59	996.59	996.59	993.91	1129.41	1225.89	1320.86	1351.37	1232.81	1351.4	1351.41	1349.22
48	907.1	996.59	970.45	996.23	907.11	996.59	907.09	996.57	1208.63	1337.53	1229.11	1343.06	1350.1	1351.41	1351.41	1351.41
49	907.02	989.8	957.72	996.51	996.59	906.98	996.59	996.33	1312.34	1296.68	1349.64	1351.31	1351.41	1351.41	1232.8	1129.38
50	996.59	992.75	996.39	996.59	907.11	996.57	996.59	990.7	1129.41	1342.95	1332.66	1351.41	1351.42	1351.42	1351.42	1232.72

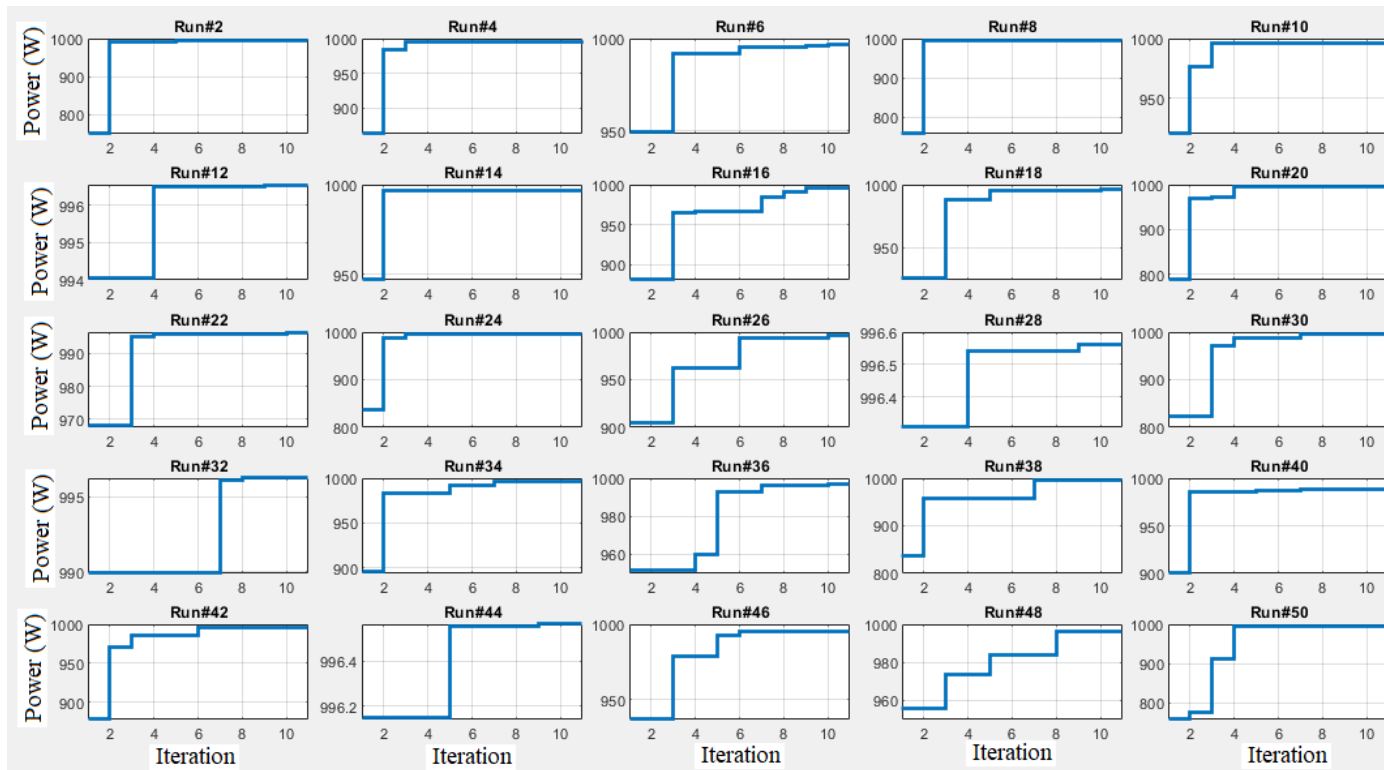


Figure A1. The PV power variation during optimization process using SFS based tracker under fifth shading scenario.

References

1. Inayat, A.; Nassef, A.M.; Rezk, H.; Sayed, E.T.; Abdelkareem, M.A.; Olabi, A.G. Fuzzy modeling and parameters optimization for the enhancement of biodiesel production from waste frying oil over montmorillonite clay K-30. *Sci. Total Environ.* **2019**, *666*, 821–827. [[CrossRef](#)] [[PubMed](#)]
2. Nassef, A.M.; Sayed, E.T.; Rezk, H.; Abdelkareem, M.A.; Rodriguez, C.; Olabi, A.G. Fuzzy-modeling with particle swarm optimization for enhancing the production of biodiesel from microalga. *Energy Sources Part A Recovery Util. Environ. Eff.* **2019**, *41*, 2094–2103. [[CrossRef](#)]
3. Choi, Y.J.; Mohamed, H.O.; Park, S.G.; Al Mayyahi, R.B.; Al-Dhaifallah, M.; Rezk, H.; Chae, K.J. Electrophoretically fabricated nickel/nickel oxides as cost effective nanocatalysts for the oxygen reduction reaction in air-cathode microbial fuel cell. *Int. J. Hydrog. Energy* **2020**, *45*, 5960–5970. [[CrossRef](#)]
4. Rezk, H.; Gomaa, M.R.; Mohamed, M.A. Energy performance analysis of on-grid solar photovoltaic system—a practical case study. *Int. J. Renew. Energy Res. (IJRER)* **2019**, *9*, 1292–1301.
5. Abdelkareem, M.A.; Sayed, E.T.; Mohamed, H.O.; Obaid, M.; Rezk, H.; Chae, K.-J. Nonprecious anodic catalysts for low-molecular-hydrocarbon fuel cells: Theoretical consideration and current progress. *Prog. Energy Combust. Sci.* **2020**, *77*, 100805. [[CrossRef](#)]
6. Nassef, A.M.; Fathy, A.; Sayed, E.T.; Abdelkareem, M.A.; Rezk, H.; Tanveer, W.H.; Olabi, A.G. Maximizing SOFC performance through optimal parameters identification by modern optimization algorithms. *Renew. Energy* **2019**, *138*, 458–464. [[CrossRef](#)]
7. Sayed, E.T.; Eisa, T.; Mohamed, H.O.; Abdelkareem, M.A.; Allagui, A.; Alawadhi, H.; Chae, K.-J. Direct urea fuel cells: Challenges and opportunities. *J. Power Sources* **2019**, *417*, 159–175. [[CrossRef](#)]
8. Rezk, H.; Alsaman, A.S.; Al-Dhaifallah, M.; Askalany, A.A.; Abdelkareem, M.A.; Nassef, A.M. Identifying optimal operating conditions of solar-driven silica gel based adsorption desalination cooling system via modern optimization. *Sol. Energy* **2019**, *181*, 475–489. [[CrossRef](#)]
9. Rezk, H.; Abdelkareem, M.A.; Ghenai, C. Performance evaluation and optimal design of stand-alone solar PV-battery system for irrigation in isolated regions: A case study in Al Minya (Egypt). *Sustain. Energy Technol. Assess.* **2019**, *36*, 100556. [[CrossRef](#)]
10. Mohamed, M.A.; Diab, A.A.Z.; Rezk, H.; Jin, T. A novel adaptive model predictive controller for load frequency control of power systems integrated with DFIG wind turbines. *Neural Comput. Appl.* **2020**, *32*, 7171–7181. [[CrossRef](#)]
11. Fathy, A.; Abd Elaziz, M.; Sayed, E.T.; Olabi, A.; Rezk, H. Optimal parameter identification of triple-junction photovoltaic panel based on enhanced moth search algorithm. *Energy* **2019**, *188*, 116025. [[CrossRef](#)]
12. Mustafa, R.J.; Gomaa, M.R.; Al-Dhaifallah, M.; Rezk, H. Environmental impacts on the performance of solar photovoltaic systems. *Sustainability* **2020**, *12*, 608. [[CrossRef](#)]
13. Diab, A.A.Z.; Rezk, H. Global MPPT based on flower pollination and differential evolution algorithms to mitigate partial shading in building integrated PV system. *Sol. Energy* **2017**, *157*, 171–186. [[CrossRef](#)]
14. Philipps, S.P.; Dimroth, F.; Bett, A.W. High-efficiency III–V multijunction solar cells. In *McEvoy's Handbook of Photovoltaics*; Academic Press: Cambridge, MA, USA, 2018; pp. 439–472.
15. Oh, G.; Kim, Y.; Lee, S.J.; Kim, E.K. Broadband antireflective coatings for high efficiency InGaP/GaAs/InGaAsP/InGaAs multi-junction solar cells. *Sol. Energy Mater. Sol. Cells* **2020**, *207*, 110359. [[CrossRef](#)]
16. Rezk, H.; Hasaneen, E.-S. A new MATLAB/Simulink model of triple-junction solar cell and MPPT based on artificial neural networks for photovoltaic energy systems. *Ain Shams Eng. J.* **2015**, *6*, 873–881. [[CrossRef](#)]
17. Fernández, E.F.; Ferrer-Rodríguez, J.P.; Almonacid, F.; Pérez-Higueras, P. Current-voltage dynamics of multi-junction CPV modules under different irradiance levels. *Sol. Energy* **2017**, *155*, 39–50. [[CrossRef](#)]
18. Or, A.B.; Appelbaum, J. Dependence of multi-junction solar cells parameters on concentration and temperature. *Sol. Energy Mater. Sol. Cells* **2014**, *130*, 234–240.
19. Segev, G.; Mittelman, G.; Kribus, A. Equivalent circuit models for triple-junction concentrator solar cells. *Sol. Energy Mater. Sol. Cells* **2012**, *98*, 57–65. [[CrossRef](#)]
20. Rezk, H.; Al-Oran, M.; Gomaa, M.R.; Tolba, M.A.; Fathy, A.; Abdelkareem, M.A.; Olabi, A.G.; El-Sayed, A.H.M. A novel statistical performance evaluation of most modern optimization-based global MPPT techniques for partially shaded PV system. *Renew. Sustain. Energy Rev.* **2019**, *115*, 109372. [[CrossRef](#)]

21. Seyedmahmoudian, M.; Mekhilef, S.; Rahmani, R.; Yusof, R.; Renani, E.T. Analytical modeling of partially shaded photovoltaic systems. *Energies* **2013**, *6*, 128–144. [[CrossRef](#)]
22. El-Helw, H.M.; Magdy, A.; Marei, M.I. A hybrid maximum power point tracking technique for partially shaded photovoltaic arrays. *IEEE Access* **2017**, *5*, 11900–11908. [[CrossRef](#)]
23. Rezk, H. An efficient single-sensor global maximum power point tracking method for partially shaded photovoltaic battery chargers. *Int. J. Energy Res.* **2019**, *43*, 8779–8789. [[CrossRef](#)]
24. Engel, E.A.; Kovalev, I.V. MPPT of a partially shaded photovoltaic module by ant lion optimizer. In *International Conference on Swarm Intelligence*; Springer: Berlin, Germany, 2016; pp. 451–457.
25. Sahu, R.K.; Shaw, B. Design of solar system by implementing ALO optimized PID based MPPT controller. *Trends Renew. Energy* **2018**, *4*, 44–55. [[CrossRef](#)]
26. Subha, R.; Himavathi, S. Mppt of PV systems under partial shaded conditions using flower pollination algorithm. In Proceedings of the 2017 IEEE International Conference on Innovations in Electrical, Electronics, Instrumentation and Media Technology (Iceimt), Coimbatore, India, 3–4 February 2017; pp. 206–210.
27. Das, N.; Wongsodihardjo, H.; Islam, S. Modeling of multi-junction photovoltaic cell using MATLAB/Simulink to improve the conversion efficiency. *Renew. Energy* **2015**, *74*, 917–924. [[CrossRef](#)]
28. Ram, J.P.; Rajasekar, N. A new global maximum power point tracking technique for solar photovoltaic (PV) system under partial shading conditions (PSC). *Energy* **2017**, *118*, 512–525.
29. Ajiatmo, D.; Robandi, I. A hybrid fuzzy logic controller-firefly algorithm (FLC-FA) based for MPPT photovoltaic (PV) system in solar car. In Proceedings of the 2016 IEEE International Conference on Power and Renewable Energy (ICPRE), Shanghai, China, 21–23 October 2016; pp. 606–610.
30. Eltamaly, A.M.; MH Farh, H.; S Al Saud, M. Impact of PSO reinitialization on the accuracy of dynamic global maximum power detection of variant partially shaded PV systems. *Sustainability* **2019**, *11*, 2091. [[CrossRef](#)]
31. Omar, O.A.; Badra, N.M.; Attia, M.A. Enhancement of on-grid pv system under irradiance and temperature variations using new optimized adaptive controller. *Int. J. Electr. Comput. Eng.* **2018**, *8*, 2650. [[CrossRef](#)]
32. Huang, C.; Wang, L.; Yeung, R.S.-C.; Zhang, Z.; Chung, H.S.-H.; Bensoussan, A. A prediction model-guided Jaya algorithm for the PV system maximum power point tracking. *IEEE Trans. Sustain. Energy* **2017**, *9*, 45–55. [[CrossRef](#)]
33. Nguyen, B.N.; Nguyen, V.T.; Duong, M.Q.; Le, K.H.; Nguyen, H.H.; Doan, A.T. Propose a mppt algorithm based on thevenin equivalent circuit for improving photovoltaic system operation. *front. Energy Res.* **2020**, *8*, 14.
34. Xu, L.; Cheng, R.; Yang, J. A new mppt technique for fast and efficient tracking under fast varying solar irradiation and load resistance. *Int. J. Photoenergy* **2020**. [[CrossRef](#)]
35. Mohamed, M.A.; Diab, A.A.Z.; Rezk, H. Partial shading mitigation of PV systems via different meta-heuristic techniques. *Renew. Energy* **2019**, *130*, 1159–1175. [[CrossRef](#)]
36. Abdalla, O.; Rezk, H.; Ahmed, E.M. Wind driven optimization algorithm based global MPPT for PV system under non-uniform solar irradiance. *Sol. Energy* **2019**, *180*, 429–444. [[CrossRef](#)]
37. Li, X.; Wen, H.; Hu, Y.; Jiang, L. A novel beta parameter based fuzzy-logic controller for photovoltaic MPPT application. *Renew. Energy* **2019**, *130*, 416–427. [[CrossRef](#)]
38. Pilakkat, D.; Kanthalakshmi, S. An improved P&O algorithm integrated with artificial bee colony for photovoltaic systems under partial shading conditions. *Sol. Energy* **2019**, *178*, 37–47.
39. Sai, K.; Moger, T. Improved SuDoKu reconfiguration technique for total-cross-tied PV array to enhance maximum power under partial shading conditions. *Renew. Sustain. Energy Rev.* **2019**, *109*, 333–348.
40. Salimi, H. Stochastic fractal search: A powerful metaheuristic algorithm. *Knowl. Based Syst.* **2015**, *75*, 1–18. [[CrossRef](#)]

